ORNL-TM-2359

Contract No. W-7405-eng-26

METALS AND CERAMICS DIVISION

AN EVALUATION OF THE MOLTEN-SALT REACTOR EXPERIMENT HASTELLOY N SURVEILLANCE SPECIMENS — SECOND GROUP

H. E. McCoy, Jr.

FEBRUARY 1969

OAK RIDGE NATIONAL LABORATORY
Oak Ridge, Tennessee
operated by
UNION CARBIDE CORPORATION
for the
U.S. ATOMIC ENERGY COMMISSION

CONTENTS

AN EVALUATION OF THE MOLTEN-SALT REACTOR EXPERIMENT HASTELLOY N SURVEILLANCE SPECIMENS — SECOND GROUP

H. E. McCoy, Jr.

ABSTRACT

We have examined the second group of Hastelloy N surveillance samples removed from the Molten-Salt Reactor Experiment. Two rods of standard Hastelloy N were removed from the surveillance position outside the core vessel and were exposed to the nitrogen plus 2 to 5% O_2 cell environment for 11,000 hr. Metallographic examination showed that the alloy was compatible with this environment, showing only superficial oxidation and no evidence of nitriding. These samples were exposed to a thermal fluence of 1.3×10^{19} neutrons/cm^2, and the mechanical properties were altered appreciably. Both tensile and creep tests were run that showed significant changes in the mechanical properties, particularly the strain at fracture. These changes are in good agreement with those observed for materials irradiated in a helium environment in the Oak Ridge Research Reactor.

Two rods of modified Hastelloy N containing small additions of titanium and zirconium were removed from the core surveillance facility with a thermal fluence of 4.1×10^{20} neutrons/cm^2. These materials had not been annealed properly to put them in their most radiation-resistant condition, but tests on these materials indicated that they have slightly improved postirradiation mechanical properties and that their corrosion resistance is acceptable.

INTRODUCTION

The Molten-Salt Reactor Experiment is a single-region reactor that is fueled by a molten fluoride salt (65 LiF–29.1 BeF_2–5 ZrF_4–0.9 UF_4, mole %), moderated by unclad graphite, and contained by Hastelloy N (Ni–16 Mo–7 Cr–4 Fe–0.05 C, wt %). The details of the reactor design and construction can be found elsewhere.[1] We knew that the neutron environment would produce some changes in the two structural materials — graphite and Hastelloy N, and we were very confident of the compatibility of these materials with the fluoride salt. However, we needed to keep abreast of the possible development of problems within the reactor itself. For these reasons, we developed a surveillance program that would allow us to follow any changes in properties of graphite and Hastelloy N specimens as the reactor operated.

The reactor went critical on June 1, 1965, and assumed normal operation in May 1966. The first group of surveillance specimens was in the reactor from September 8, 1965, to July 28, 1966, and was removed after 8682 Mwhr of operation (designated "first group"). The results of our tests on the Hastelloy N specimens were reported previously.[2] A second set of specimens was removed from the core on May 9, 1967, after an additional 27,600 Mwhr of operation (total reactor operation was 36,247 Mwhr). These specimens were two modified alloys containing nominal 0.5% additions of titanium and zirconium. These were inserted on September 13, 1966, after the first group was removed to determine the mechanical property changes of these alloys due to irradiation and to evaluate the compatibility of these alloys with the MSRE environment. Two rods of standard Hastelloy N located outside the core and 5 in. from the vessel were removed on June 5, 1967. These specimens had been in place since the reactor began operation and were examined to determine the compatibility of the material with the MSRE cell environment (N_2 + 2–5% O_2) and the changes in the mechanical properties due to irradiation.

This report will describe the results of tests on the Hastelloy N surveillance specimens removed during May and June 1967 (designated "second group"), which includes two rods of modified (zirconium and titanium) alloys removed from the core and two rods of standard Hastelloy N removed from outside the core vessel.

---

[1]R. C. Robinson, MSRE Design and Operations Report, Pt. 1, Description of Reactor Design, ORNL-TM-728 (January 1965).

[2]H. E. McCoy, Jr., An Evaluation of the Molten-Salt Reactor Experiment Hastelloy N Surveillance Specimen — First Group, ORNL-TM-1997 (November 1967).

EXPERIMENTAL DETAILS

Surveillance Assembly

The core surveillance assembly was designed by W. H. Cook and others, and the details have been reported.[3] The facility is shown pictorially and schematically in Fig. 1. The specimens are arranged in three stringers. Each stringer is about 62 in. long and consists of two Hastelloy N rods and a graphite section made up of various pieces that are joined by pinning and tongue-and-groove joints. The Hastelloy N rod is periodically reduced to 0.125 in. in diameter and can be cut into small tensile specimens after it is removed from the reactor. Three stringers are joined together so that they can be separated in a hot cell and reassembled with one or more new stringers for reinsertion into the reactor. The assembled stringers fit into a perforated Hastelloy N basket that is inserted into an axial position about 2.8 in. from the core center line.

When the basket was removed on July 28, 1966, some of the specimens were bent, and the entire assembly had to be replaced.[4] Slight modifications in the design were made, and the assembly was removed recently and found to be in excellent condition.[5]

A control facility is associated with the surveillance program. It utilizes a "fuel salt" containing depleted uranium in a static pot that is heated electrically. The temperature is controlled by the MSRE computer so that the temperature matches that of the reactor. Thus, these specimens are exposed to conditions the same as those in the reactor except for the static salt and the absence of a neutron flux.

---

[3]W. H. Cook, MSR Program Semiann. Progr. Rept. Aug. 31, 1965, ORNL-3872, p. 87.

[4]W. H. Cook, MSR Program Semiann. Progr. Rept. Aug. 31, 1966, ORNL-4037, p. 97.

[5]W. H. Cook, "MSRE Materials Surveillance Program," Metals and Ceramics Div. Ann. Progr. Rept. June 30, 1967, ORNL-4170, pp 192–195.

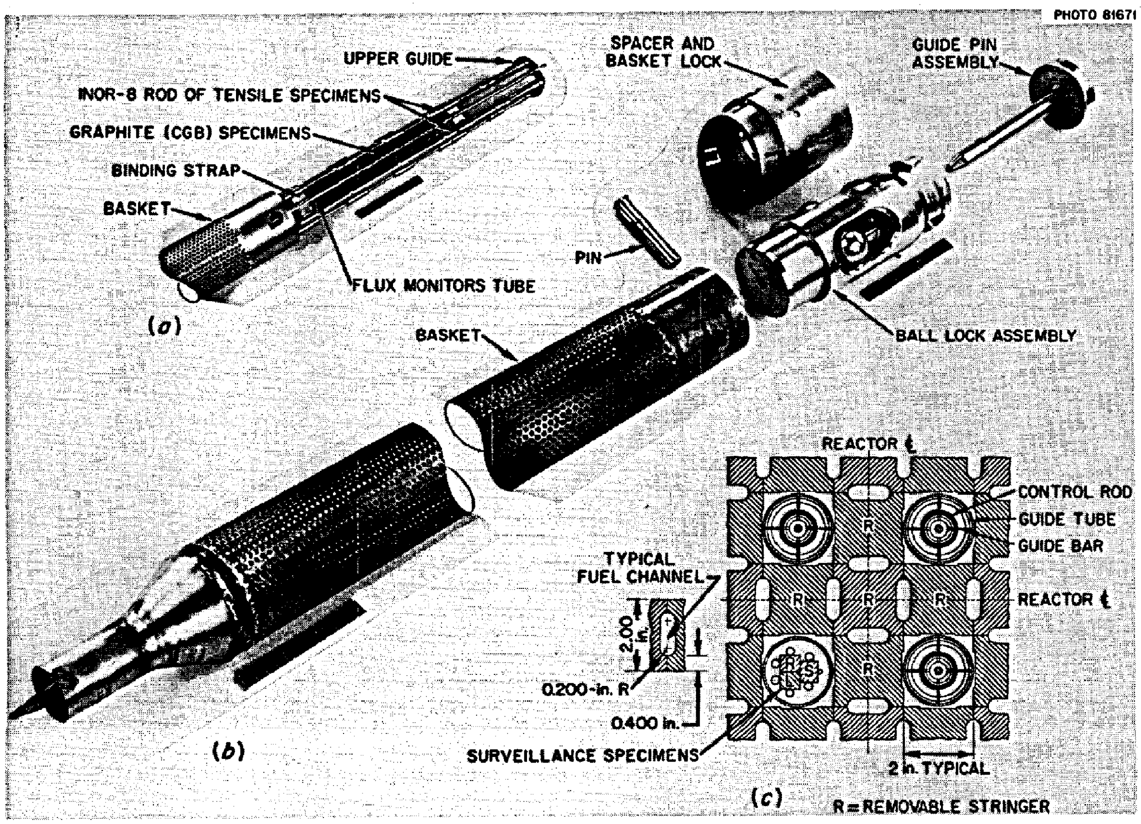

Fig. 1. Molten-Salt Reactor Experiment Core Surveillance Fixture.

There is another surveillance facility for Hastelloy N located outside the core in a vertical position about 5 in. from the vessel (Fig. 2). These specimens are exposed to the cell environment (N_2 + 2–5% O_2).

Materials

The compositions of the two heats of standard Hastelloy N are given in Table 1. These heats were air melted by Materials Systems Division of Union Carbide Corporation. Heat 5085 was used for making the cylindrical portion, and heat 5065 was used for the top and bottom heads of the MSRE vessel. These materials were given a mill anneal of 1 hr at 1177°C and a final anneal of 2 hr at 900°C at ORNL after fabrication.

The chemical compositions of the two modified alloys are given in Table 1. The modifications in composition were made principally to improve the alloy's resistance to radiation damage and to bring about

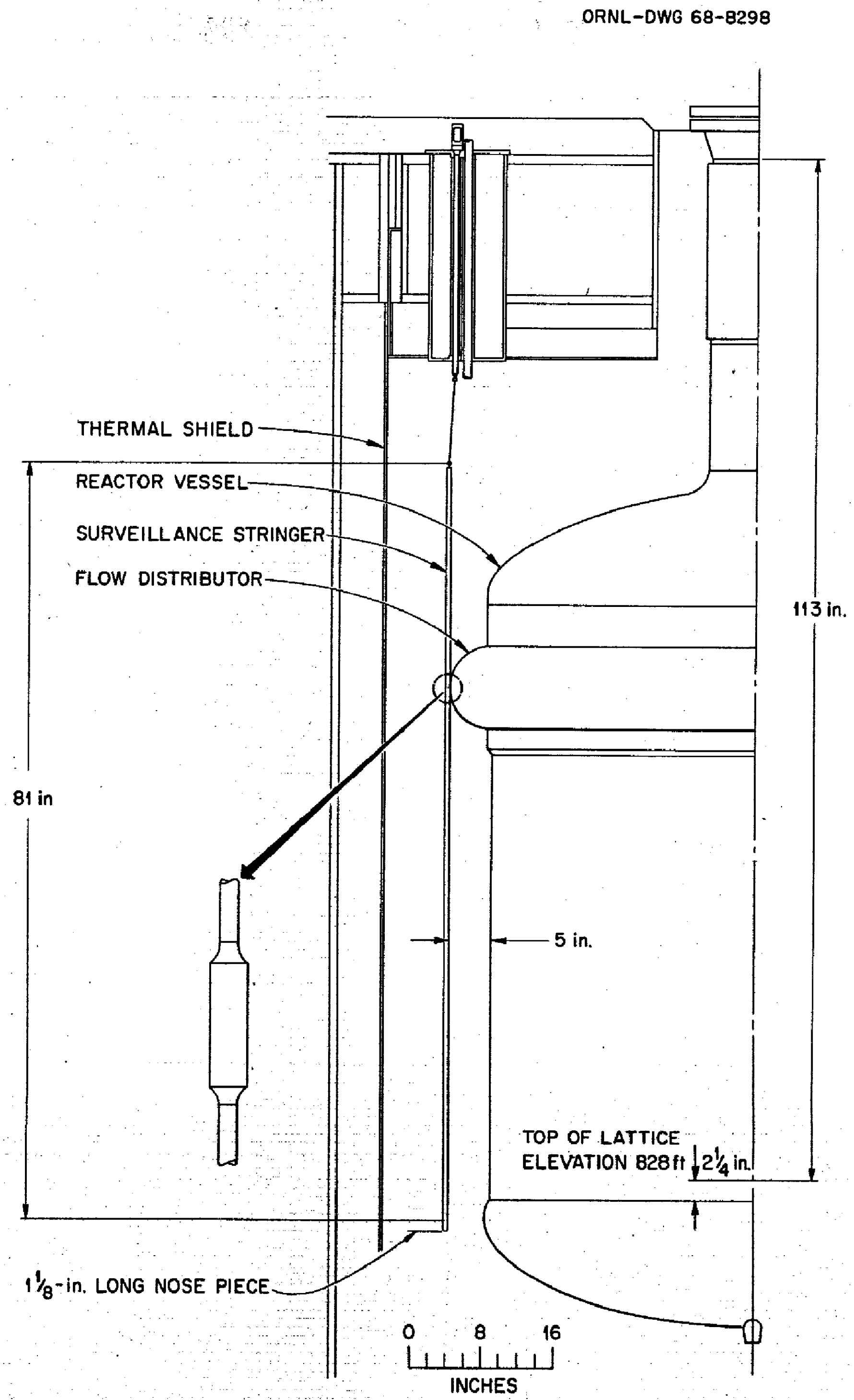

Fig. 2. Molten-Salt Reactor Experiment Surveillance Facility Outside the Reactor Vessel.

Table 1. Chemical Composition of Surveillance Heats

Element	Analysis, wt %			
	Heat 5065	Heat 5085	Heat 21545	Heat 21554
Cr	7.2	7.3	7.18	7.39
Fe	3.9	3.5	0.034	0.097
Mo	16.5	16.7	12.0	12.4
C	0.065	0.052	0.05	0.065
Si	0.60	0.58	0.015	0.010
Co	0.08	0.15		
W	0.04	0.07		
Mn	0.55	0.67	0.29	0.16
V	0.22	0.20		
P	0.004	0.0043	0.001	0.004
S	0.007	0.004	< 0.002	< 0.002
Al	0.01	0.02	0.02	0.03
Ti	0.01	< 0.01	0.49	0.003
Cu	0.01	0.01		
O	0.0016	0.0093	0.0002	< 0.0001
N	0.011	0.013	< 0.0001	0.0005
Zr				0.35
	Analysis, ppm			
B	24, 37, 20, 10	38	2	2

general improvements in the fabricability, weldability, and ductility.[6] These alloys were small 100-lb heats made by vacuum melting by Special Metals Corporation. They were finished to 1/2-in. plate containing 40% cold work. We used slightly different procedures for obtaining the 1/4-in.-diam × 62-in.-long rods required for the surveillance assembly as indicated by their fabrication history:

<u>Heats 5065 and 5085</u>

1. Materials available as 1 1/8- and 9/16-in. plate, respectively. Mill annealed 1 hr at 1177°C.
2. Segments of 1/4-in.-diam rod machined.
3. Reduced sections turned in rods.
4. Segments welded together to make 62-in.-long rods.
5. Annealed 2 hr at 900°C.

<u>Heat 21545</u>

1. Material available as plates 1/2 in. thick × 3 in. wide × 12 in. long. Fabricated with 40% residual cold work.
2. Strips 1/2 × 1/2 × 12 in. cut from plate.
3. Strips machined to 1/4-in.-diam rods.
4. Rods were annealed 100 hr at 871°C.
5. Rods welded together.
6. Specimens machined.

<u>Heat 21554</u>

1. Material available as plates 1/2 in. thick × 3 in. wide × 12 in. long. Fabricated with 40% residual cold work.
2. Plate worked at 871°C to 0.3 in. thickness.
3. Strips 0.3 × 0.3 × 20 in. cut.
4. Strips machined to 1/4 in.-diam rods.
5. Rods were annealed 100 hr at 871°C.
6. Rods were straightened.
7. Rods reannealed 100 hr at 871°C.
8. Rods welded together.
9. Specimens machined.

---

[6] H. E. McCoy, Jr., and J. R. Weir, Jr., <u>Materials Development for Molten-Salt Breeder Reactors</u>, ORNL-TM-1854 (June 1967).

Both procedures resulted in a very fine grain size (ASTM grain size 7 to 9).

Test Specimens

The surveillance rods inside the core are 62 in. long and those outside the vessel are 81 in. long. They both are 1/4 in. in diameter with reduced sections 1/8 in. in diameter by 1 1/8 in. long. After removal from the reactor, the rods are sawed into small mechanical property specimens having a gage section 1/8 in. in diameter by 1 1/8 in. long.

The first rods were machined in small segments (approx 11 1/2 in. long) and welded together. An improvement in this technique has been made that allows the entire rod to be machined as a unit (see Fig. 3).

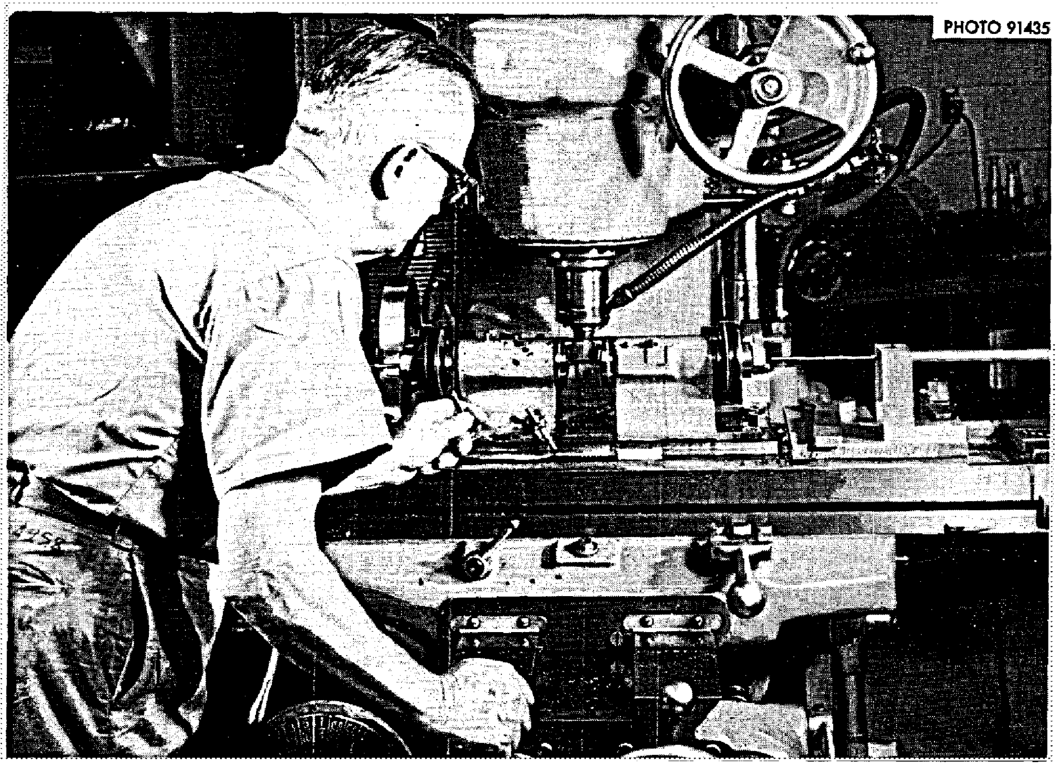

Fig. 3. Fabrication of Hastelloy N Surveillance Rods.

A milling machine is used with a cutter ground to the shape of the gage length, including the radius where the gage length blends into the full 1/4 in. diameter of the rod. The rod is held in position and rotated while being fed into the milling cutter. The rod then requires only a light hand polishing of the gage sections to obtain the desired surface finish. This procedure is quicker, cheaper, and requires less handling of the relatively fragile rods than the previous method of making the rods from segments.

Irradiation Conditions

The irradiation conditions in the core were described in detail previously.[7] These measurements were repeated for the second group of core specimens and found to be in excellent agreement. The specimens outside the core are exposed to the cell environment of N_2 + 2–5% O_2. The pertinent temperature and flux data are summarized in Table 2.

Testing Techniques

The laboratory creep-rupture tests were run in conventional creep machines of the dead-load and lever-arm types. The strain was measured by a dial indicator that showed the total movement of the specimen and part of the load train. The zero strain measurement was taken immediately after the load was applied. The temperature accuracy was ±0.75%, the guaranteed accuracy of the Chromel-P–Alumel thermocouples used.

The postirradiation creep-rupture tests were run in lever-arm machines that were located in hot cells. The strain was measured by an extensometer with rods attached to the upper and lower specimen grips. The relative movement of these two rods was measured by a linear differential transformer, and the transformer signal was recorded. The accuracy of the strain measurements is difficult to determine. The

[7]H. E. McCoy, Jr., An Evaluation of the Molten-Salt Reactor Experiment Hastelloy N Surveillance Specimen — First Group, ORNL-TM-1997 (November 1967).

Table 2. Surveillance Program of the MSRE

	Group 1[a]	Group 2	
	Core Standard Hastelloy N	Core Modified Hastelloy N	Vessel Standard Hastelloy N
Date inserted	9/8/65	9/13/66	8/24/65
Date removed	7/28/66	5/9/67	6/5/67
Mwhr on MSRE at time of insertion	0.0066	8682	0
Mwhr on MSRE at time of removal	8682	36,247	36,247
Temperature, °C	650 ± 10	650 ± 10	650 ± 10
Time at temperature, hr	4800	5500	11,000
Peak fluence, neutrons/cm^2			
Thermal (<0.876 ev)	1.3×10^{20}	4.1×10^{20}	1.3×10^{19}
Epithermal (>0.876 ev)	3.8×10^{20}	1.2×10^{21}	2.5×10^{19}
(>50 kev)	1.2×10^{20}	3.7×10^{20}	2.1×10^{19}
(>1.22 Mev)	3.1×10^{19}	1.0×10^{20}	5.5×10^{18}
(>2.02 Mev)	1.6×10^{19}	0.5×10^{20}	3.0×10^{18}
Peak flux, neutrons cm^{-2} sec^{-1} mw^{-1}			
Thermal (<0.876 ev)	4.1×10^{12} (b,c)	4.1×10^{12} (b,c)	1.0×10^{11} (b)
Epithermal (>0.876 ev)	1.2×10^{13} (c)	1.2×10^{13} (c)	1.9×10^{11} (b,c)
(>50 kev)	3.7×10^{12} (c)	3.7×10^{12} (c)	1.6×10^{11} (c)
(>1.22 Mev)	1.0×10^{12} (b,c)	1.0×10^{12} (b,c)	4.2×10^{10} (b)
(>2.02 Mev)	0.5×10^{12} (b,c)	0.5×10^{12} (b,c)	2.3×10^{10} (b)

[a]Revised for full power operation at 8 Mw.

[b]Experimentally determined.

[c]Calculated.

extensometer (mechanical and electrical portions) produced measurements that could be read to about ±0.02% strain; however, other factors (temperature changes in the cell, mechanical vibrations, etc.) probably combined to give an overall accuracy of ±0.1% strain. This is considerably better than the specimen-to-specimen reproducibility that one would expect for relatively brittle materials. The temperature measuring and control system was the same as that used in the laboratory with only one exception. In the laboratory, the control system was stabilized at the desired temperature by use of a recorder with an expanded scale. In the tests in the hot cells, the control point was established by setting the controller without the aid of the expanded-scale recorder. This error and the thermocouple accuracy combine to give a temperature uncertainty of about ±1%.

The tensile tests were run on Instron Universal Testing Machines. The strain measurements were taken from the crosshead travel.

The test environment was air in all cases. Metallographic examination showed that the depth of oxidation was small, and we feel that the environment did not appreciably influence the test results.

EXPERIMENTAL RESULTS

Visual and Metallographic Examination

W. H. Cook was in charge of the disassembly of the surveillance fixture. Although some difficulties were encountered previously,[8] the design modifications were successful and the assembly was in excellent mechanical condition when removed. The graphite and Hastelloy N surfaces were very clean with markings such as numbers and tool marks very clear. The Hastelloy N was discolored very slightly. Representative photographs are shown in Fig. 4.

[8] W. H. Cook, "MSRE Materials Surveillance Program," Metals and Ceramics Div. Ann. Progr. Rept. June 30, 1967, ORNL-4170, pp. 192–195.

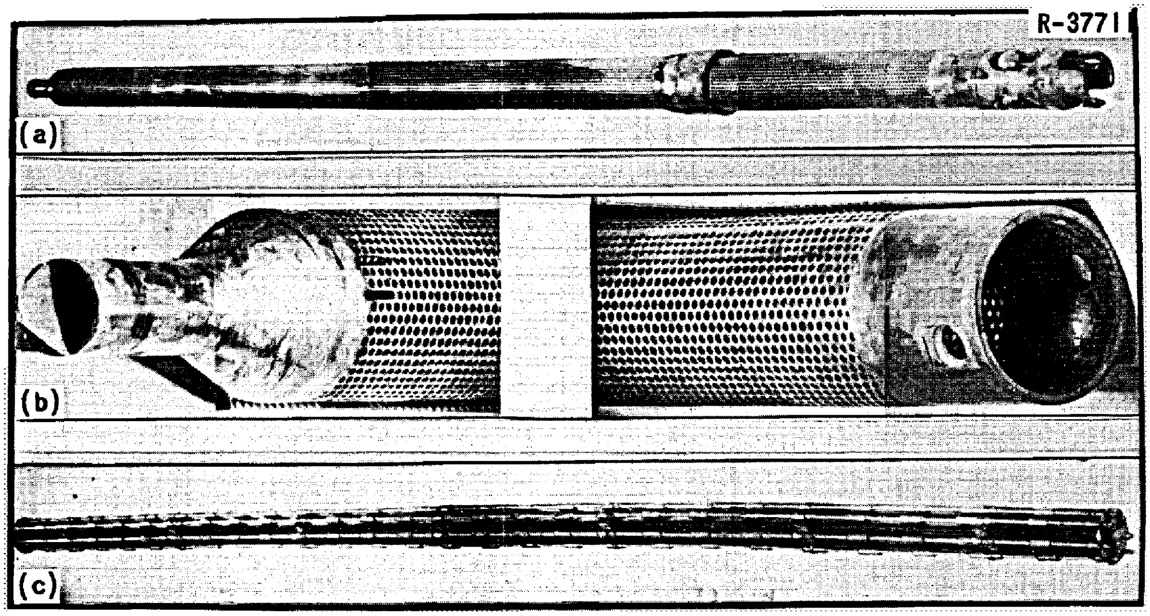

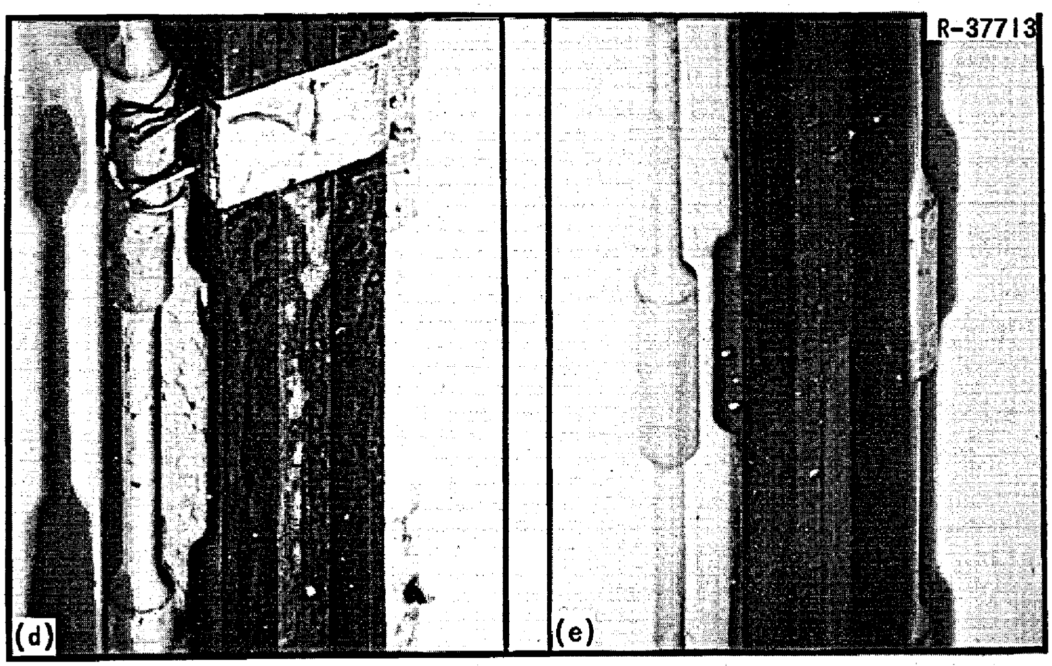

Fig. 4. Core Surveillance Specimens Removed on May 9, 1967. (a) Outside of protective Hastelloy N basket. (b) Close-ups of the top and bottom of the basket. (c) Surveillance stringer after removal from the basket (curvature due to optical system in the hot cell). (d and e) Close-ups of the surveillance specimens showing the high reflectivity of the metal and graphite specimens. A few beads of salt remain on the graphite.

Small pieces of the modified alloys removed from the core were examined metallographically. Photomicrographs of heat 21554 (zirconium modified) are shown in Fig. 5. The bulk material is characterized by a very fine grain size and small inhomogeneous areas that were found to be essentially pure molybdenum (probably a result of poor melting practice). The as-polished sample shows some very slight microstructural changes near the surface to a depth of 1 to 2 mils. Similar micrographs are shown in Fig. 6 for heat 21545 (titanium modified). The grain size of this material is slightly smaller, but the other features are quite similar to those observed for heat 21554.

A small piece of the basket that contained the surveillance assembly was examined metallographically. The basket was made from perforated Hastelloy N sheet. The entire surface exposed to the salt is characterized by the photomicrographs shown in Fig. 7. Small grains appeared to be almost dislodged from the surface [Fig. 7(a)]. After etching, a fine precipitate was revealed near the surface to a depth of 1 to 2 mils. We examined the material used in fabricating the basket; the microstructure is shown in Fig. 8. There is some precipitate near the surface, but not in the quantities observed in Fig. 7. We aged a piece of the material for 1000 hr at 650°C (basket in MSRE was exposed 5500 hr) and found that the quantity of precipitate increased (Fig. 9). However, we were not able to dislodge any grains near the surface even after a very sharp cold bend.

A sample from the basket was sent to N. R. Stalica, Argonne National Laboratory, for microprobe studies. This investigator found that the precipitates contained silicon and oxygen in large concentrations and suggested that they were SiO_2. Our studies on the unirradiated specimens showed that the precipitates are metal-silicon compounds. We are continuing to investigate this point, but presently feel that the precipitates are probably related to surface contamination of the basket during fabrication. The silicon-rich contaminant should be dissolved during the post-fabrication anneal (approx 1177°C) given the basket and subsequently precipitate while in service at 650°C.

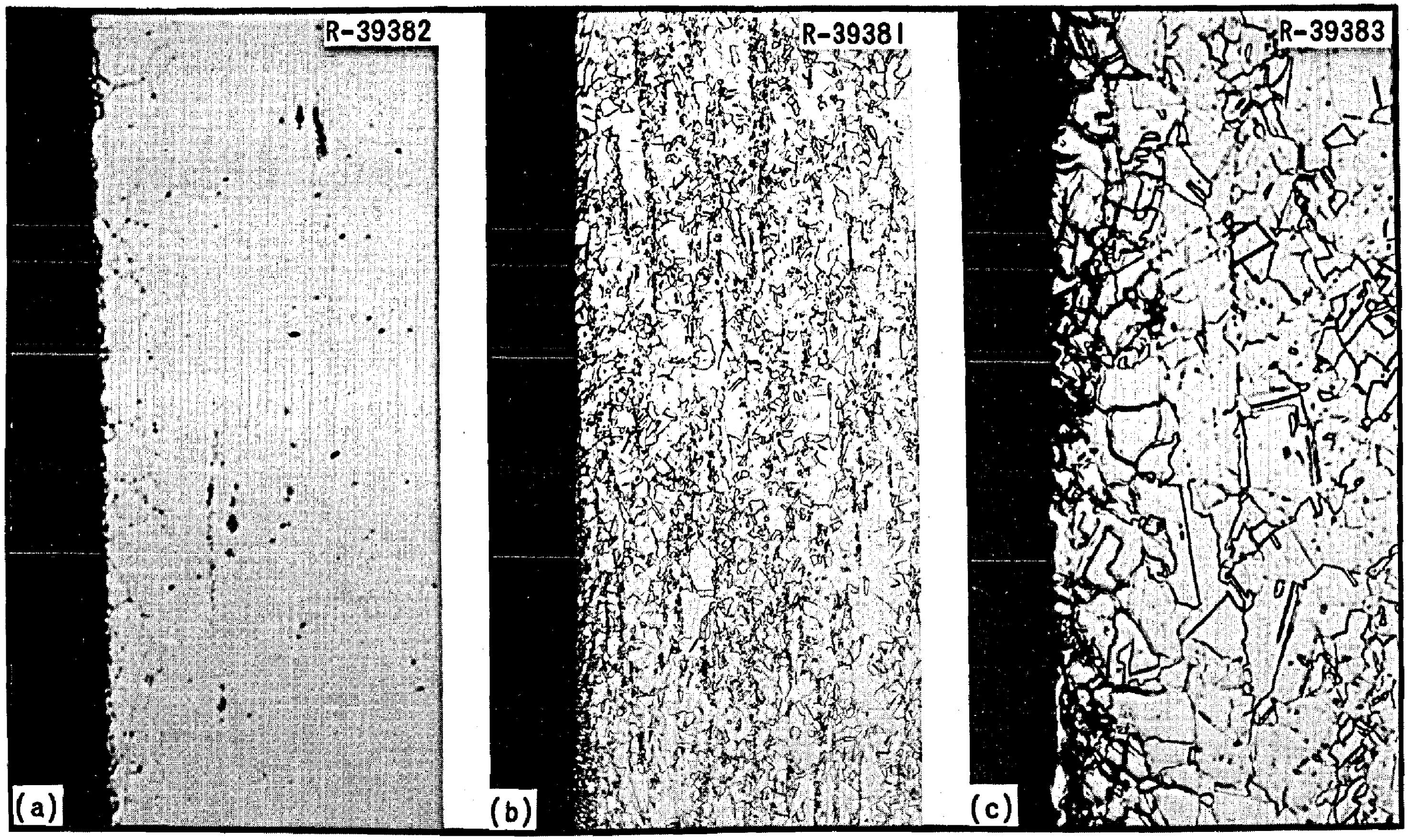

Fig. 5. Photomicrographs of Zirconium-Modified Hastelloy N (Heat 21554) Removed from the MSRE after 5500 hr at 650°C. Edge exposed to flowing salt. (a) As polished. 500×. (b) Etchant: Aqua regia. 100×. (c) Etchant: Aqua regia. 500×.

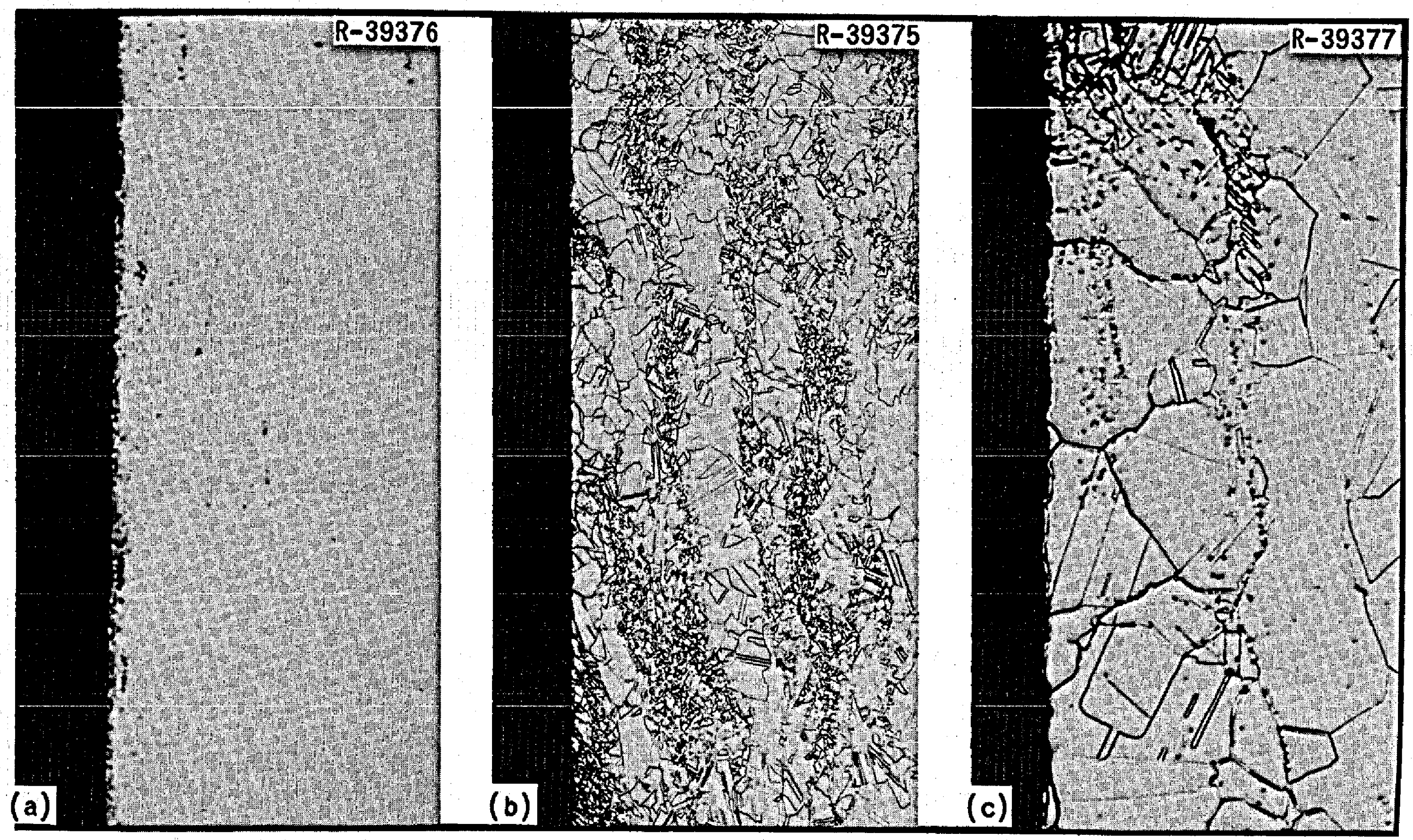

Fig. 6. Photomicrographs of Titanium-Modified Hastelloy N (Heat 21545) Removed from the MSRE after 5500 hr at 650°C. Edge exposed to flowing salt. (a) As polished. 500×. (b) Etchant: Aqua regia. 100×. (c) Etchant: Aqua regia. 500×.

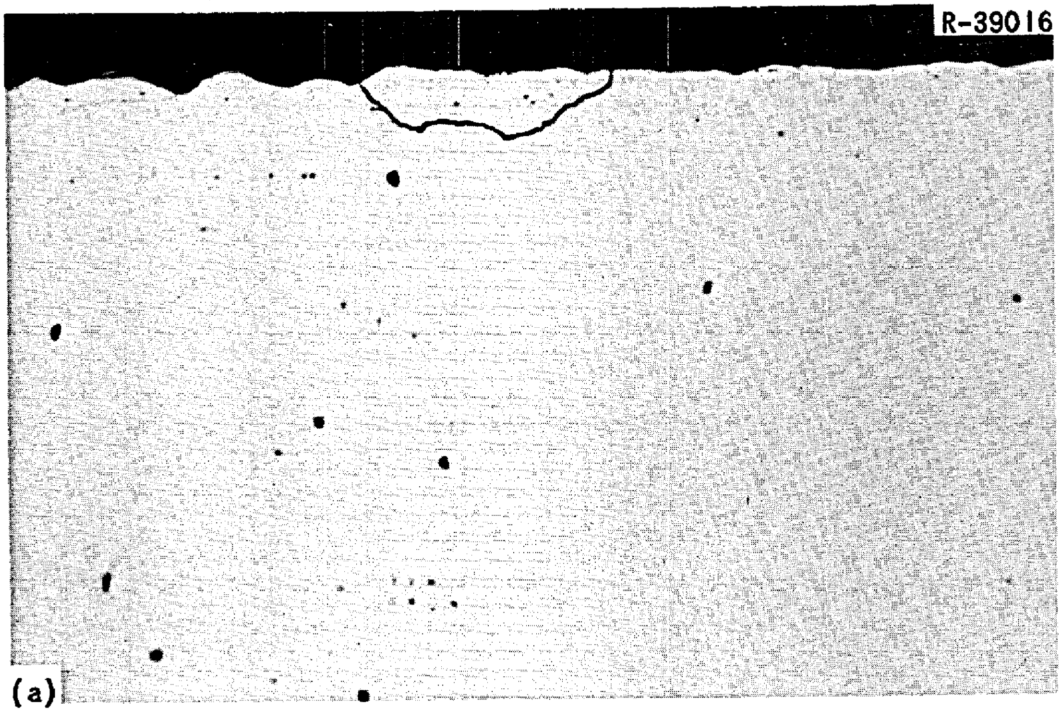

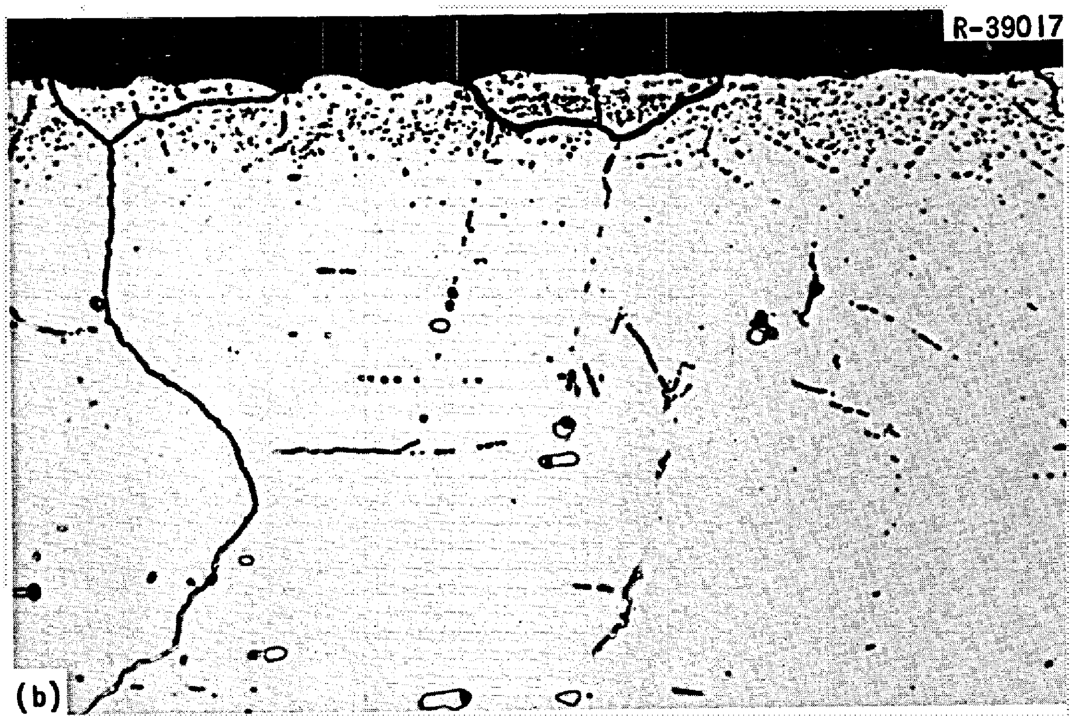

Fig. 7. Photomicrographs of the Edge of the Surveillance Basket Removed from the MSRE after 5500 hr at 650°C. 500×. (a) As polished. Note the grain near the surface that seems almost dislodged. (b) Etchant: Aqua regia. Same area as shown in (a). Note the fine precipitate near the surface.

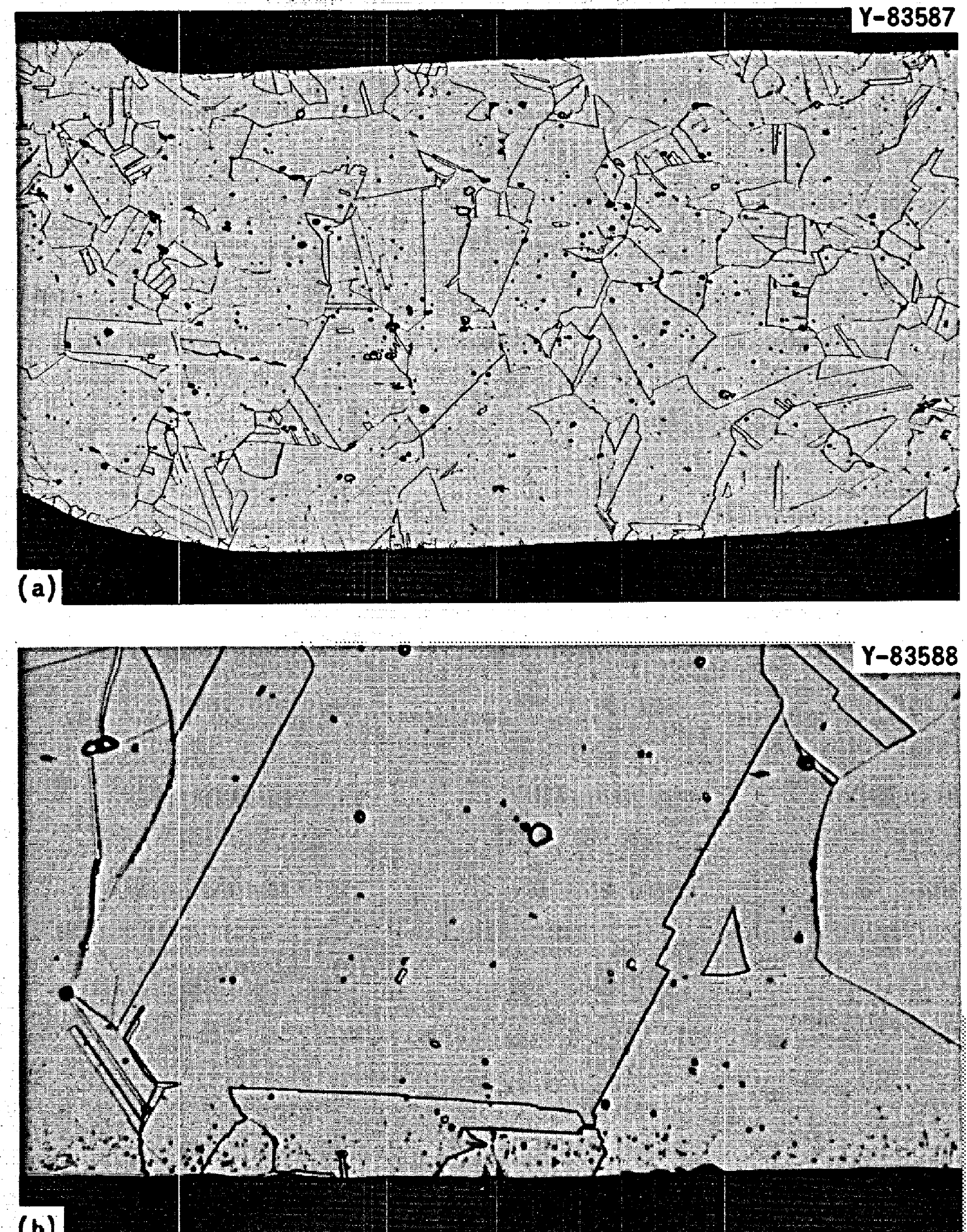

Fig. 8. Photomicrographs of the Material Used in Making the Surveillance Basket. The final processing step was a 1-hr anneal at 1177°C. Etchant: Glyceria regia. (a) 100×. (b) 500×.

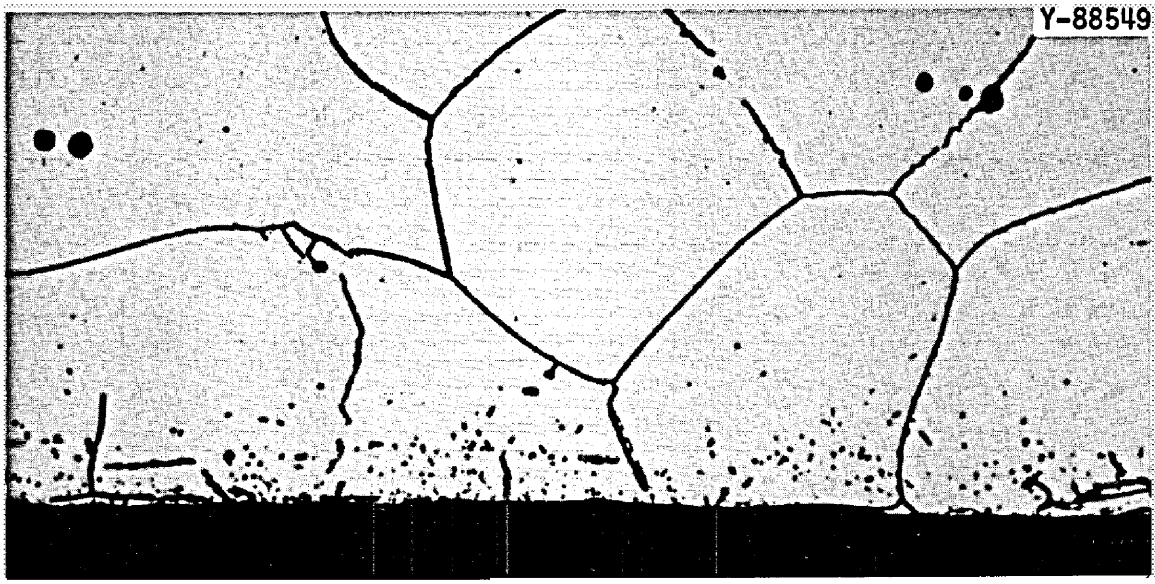

Fig. 9. Photomicrograph of the Material Used to Make the Surveillance Basket after a 1-hr Anneal at 1177°C and Aging for 1000 hr at 650°C. 750×. Etchant: Glyceria regia.

Small pieces of the standard Hastelloy N specimens that had been exposed to the MSRE cell environment for 11,000 hr were examined. Microstructures of heat 5085 are shown in Fig. 10. A thin oxide is present on the surface and some changes in microstructures occur to a depth of about 3 mils. The sample examined from heat 5085 was from a welded region. As shown in Fig. 11, the depth of attack seemed to be somewhat greater, but the reaction layer is very shallow. Neither specimen showed any evidence of nitrogen absorption from the cell environment.

Mechanical Property Data — Standard Hastelloy N

The postirradiation tensile properties of heat 5065 are summarized in Table 3. The fracture strains are plotted as a function of test temperature in Fig. 12. There are significant reductions in the fracture strain at 25°C and above 500°C. The properties of heat 5085 are given in Table 4. The fracture strains are plotted in Fig. 13 and are very similar to those noted for heat 5065. The strain at fracture for both heats is reduced above about 400°C by reducing the strain rate.

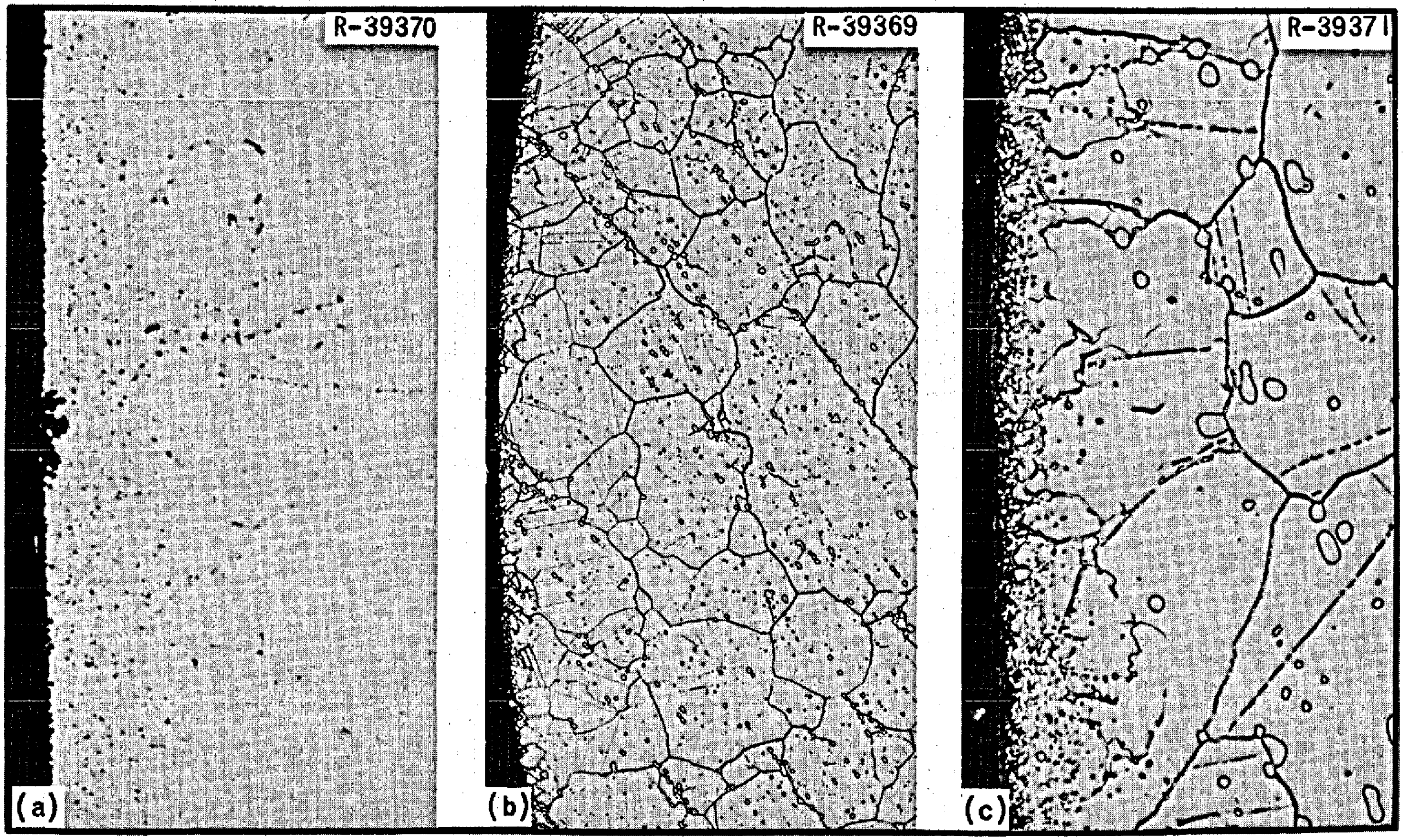

Fig. 10. Photomicrographs of a 1/4-in.-diam Rod of Standard Hastelloy N (Heat 5085) Exposed to the MSRE Cell Environment of N_2 + 2–5% O_2 for 11,000 hr at 650°C. (a) As polished. 500×. (b) Etchant: Aqua regia. 100×. (c) Etchant: Aqua regia. 500×.

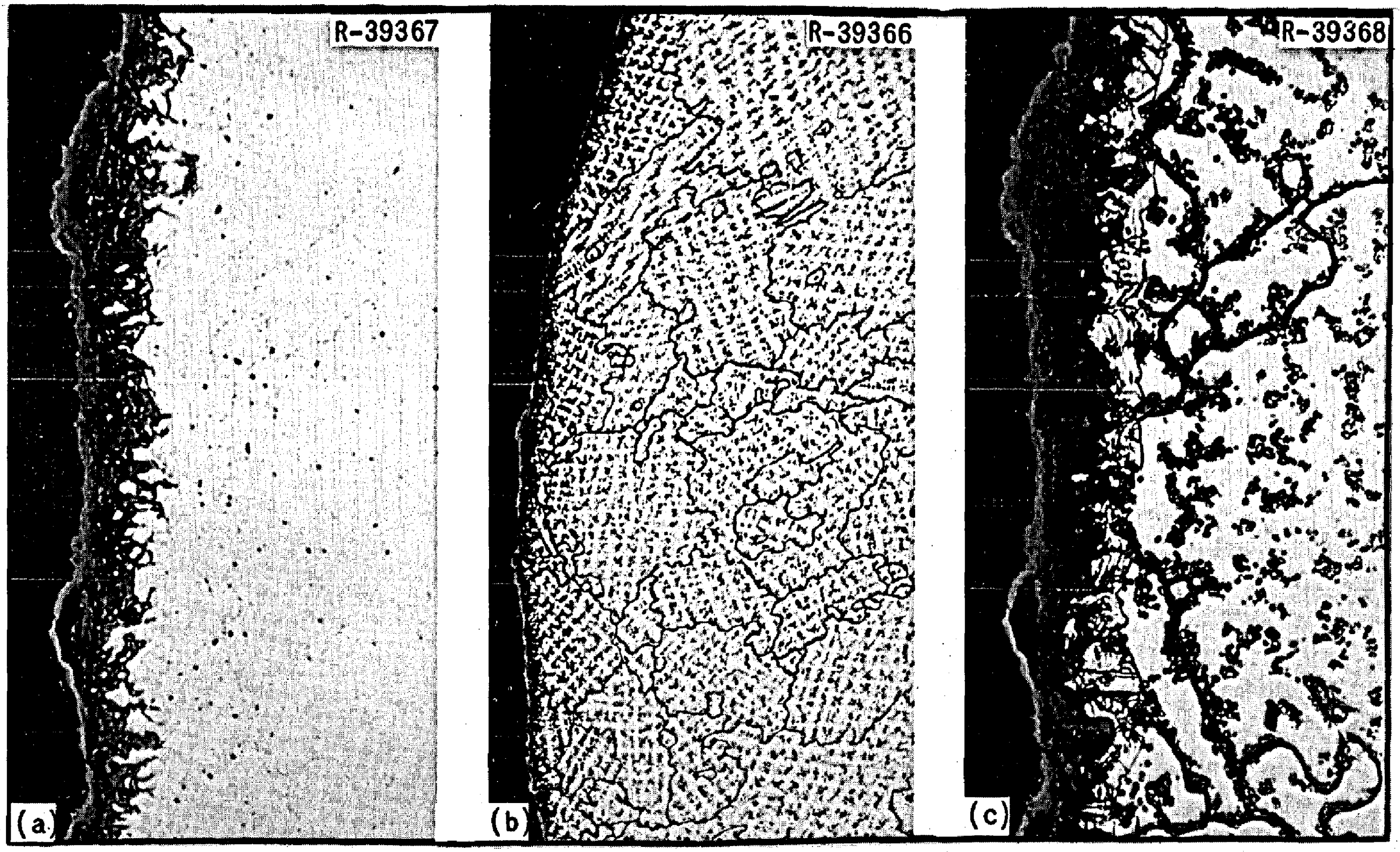

Fig. 11. Photomicrographs of a 1/4-in.-diam Rod of Standard Hastelloy N (Heat 5065) Exposed to the MSRE Cell Environment of N_2 + 2–5% O_2 for 11,000 hr at 650°C. The cross section viewed is a weld made in joining small segments to make the single surveillance rod. (a) As polished. 500×. (b) Etchant: Aqua regia. 100×. (c) Etchant: Aqua regia. 500×.

Table 3. Results of Tensile Tests on MSRE Surveillance Specimens — Heat 5065

Specimen Number	Test Temperature (°C)	Strain Rate (min^{-1})	Stress, psi		Elongation, %		Reduction in Area (%)	True Fracture Strain (%)
			Yield	Ultimate	Uniform	Total		
9011	25	0.050	58,500	110,500	34.1	34.6	26.93	31
9012	200	0.050	43,100	111,000	61.2	63.2	46.14	62
9014	400	0.050	38,900	102,300	59.0	63.0	43.75	58
9033	400	0.002	39,100	106,000	56.6	57.7	43.75	58
9015	450	0.050	38,200	100,200	56.5	58.8	35.48	44
9032	450	0.002	38,100	102,700	52.0	56.0	38.53	49
9016	500	0.050	40,200	104,300	55.5	57.7	31.66	38
9013	500	0.002	39,500	98,900	48.6	50.0	39.58	50
9017	550	0.050	39,800	100,900	51.5	52.9	34.40	42
9022	550	0.002	36,600	83,000	27.3	28.0	24.75	28
9018	600	0.050	38,100	92,000	34.8	35.8	25.93	30
9023	600	0.002	36,200	72,900	22.7	23.0	22.02	25
9019	650	0.050	40,700	99,200	25.3	25.8	22.73	26
9024	650	0.002	33,600	54,200	11.1	11.4	10.89	12
9020	760	0.050	31,100	56,800	6.8	7.3	14.79	16
9025	760	0.002	30,600	31,400	1.3	3.6	4.74	5
9021	850	0.050	29,500	43,400	6.2	7.5	4.78	5
9026	850	0.002	25,300	25,400	1.0	2.8	3.21	3

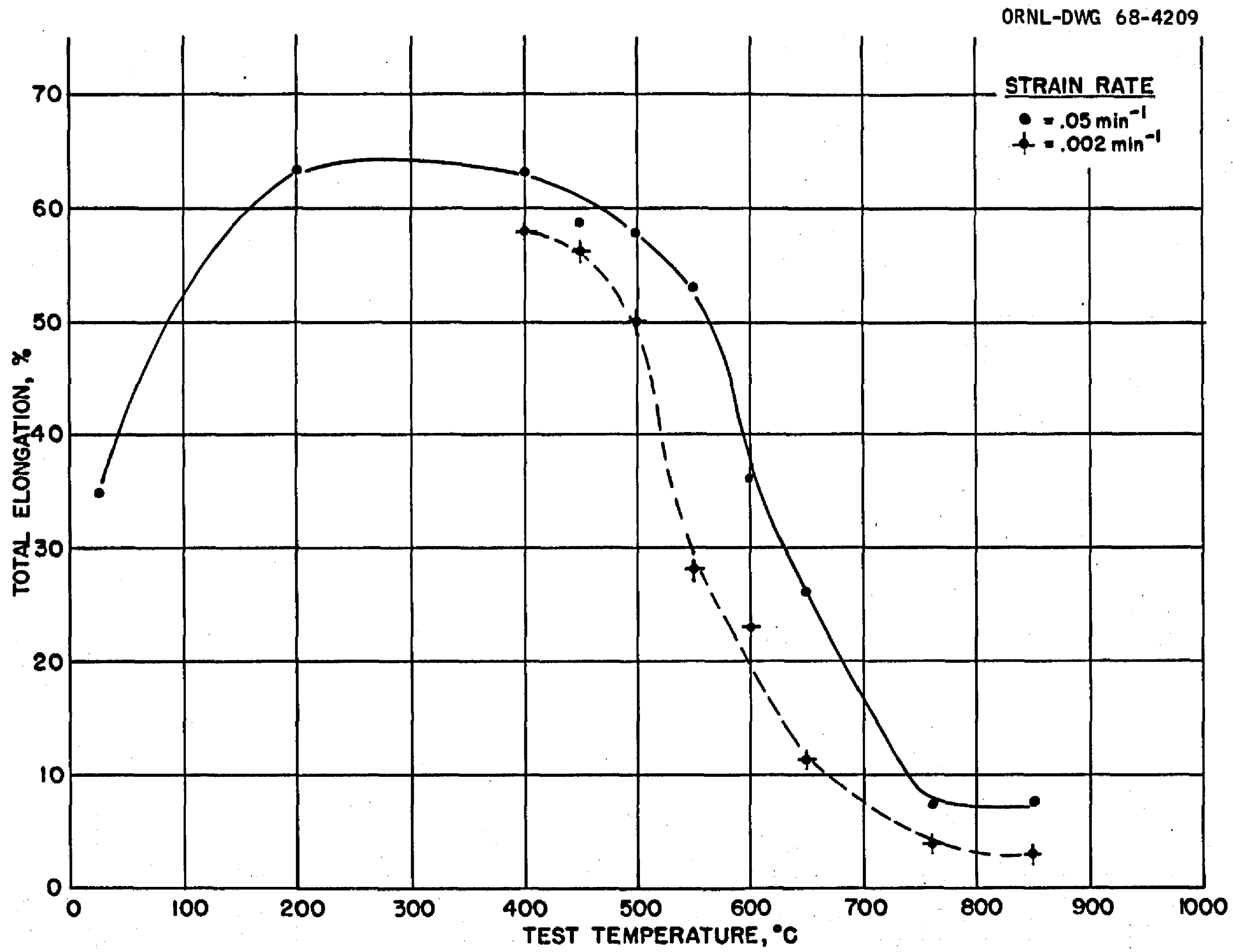

Fig. 12. Variation of Ductility with Temperature for MSRE Surveillance Specimens. Heat 5065. Thermal fluence was 1.3×10^{19} neutrons/cm^2.

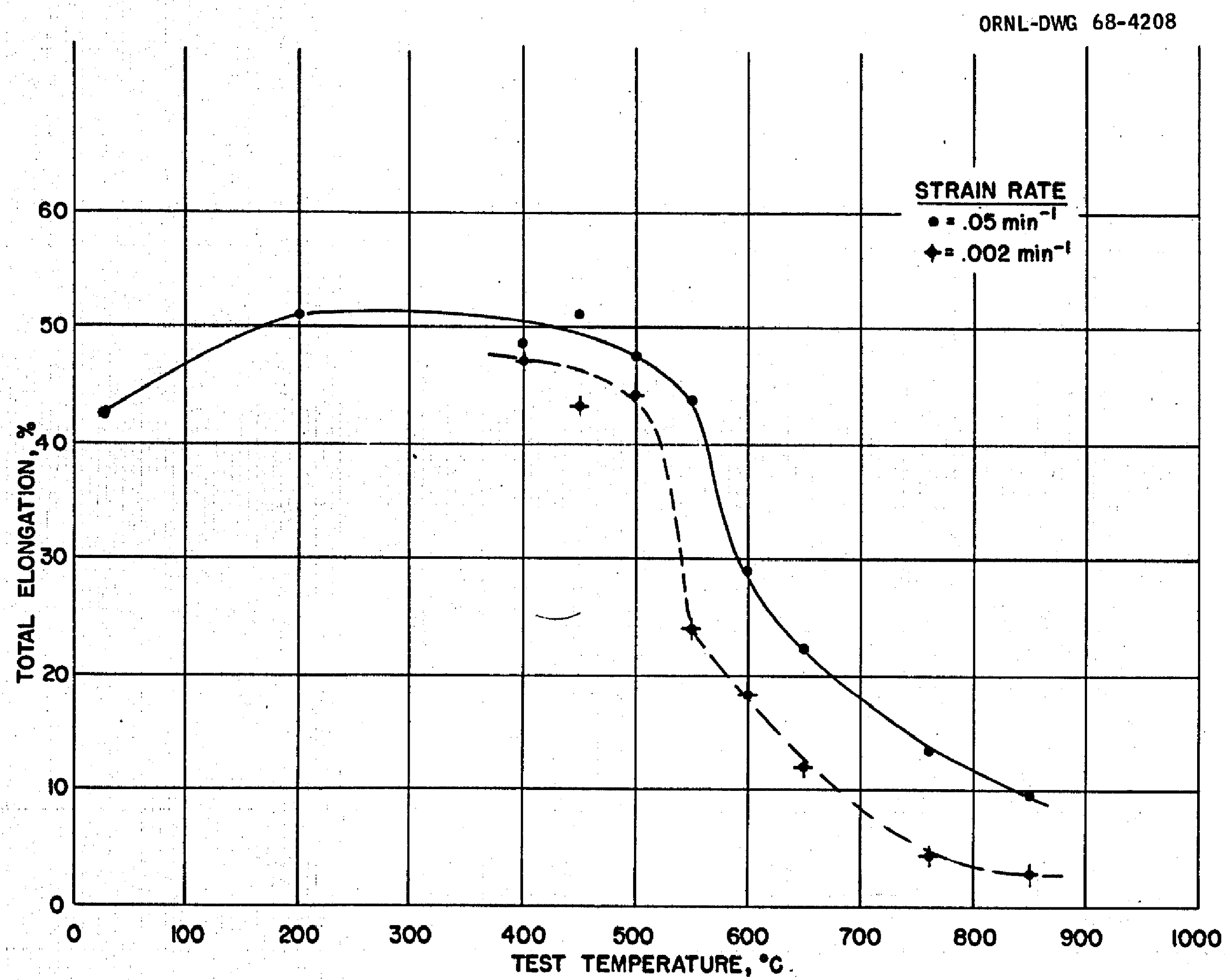

Fig. 13. Variation of Ductility with Temperature for MSRE Surveillance Specimens. Heat 5085. Thermal fluence was 1.3×10^{19} neutrons/cm^2.

Table 4. Results of Tensile Tests on MSRE Surveillance Specimens — Heat 5085

Specimen Number	Test Temperature (°C)	Strain Rate (min^{-1})	Stress, psi		Elongation, %		Reduction in Area (%)	True Fracture Strain (%)
			Yield	Ultimate	Uniform	Total		
9047[a]	25	0.050	64,000	114,900	42.5	42.5	24.14	28
9049	200	0.050	39,000	102,700	49.8	51.0	39.30	50
9050	400	0.050	37,600	96,800	47.9	48.7	37.03	46
9069	400	0.002	36,600	95,300	46.3	46.9	32.88	40
9052	450	0.050	36,300	95,200	50.7	51.2	33.78	41
9070	450	0.002	36,400	92,700	42.5	43.1	26.93	31
9053	500	0.050	36,100	92,600	47.5	47.5	33.48	41
9058	500	0.002	38,100	78,700	23.3	24.4	21.31	24
9054	550	0.050	35,500	89,800	42.8	43.8	25.93	30
9060	550	0.002	34,800	75,200	23.4	24.1	21.31	24
9055	600	0.050	34,800	77,700	28.5	29.0	26.93	31
9061	600	0.002	33,700	64,600	17.5	18.2	23.35	27
9056	650	0.050	35,400	70,600	20.9	22.4	22.02	25
9062	650	0.002	32,200	43,500	11.2	12.0	5.54	6
9057	760	0.050	29,000	49,700	12.6	13.5	12.49	13
9071	760	0.002	29,000	32,400	1.9	4.3	1.62	2
9059	850	0.050	27,800	37,900	6.3	9.7	7.84	8
9068	850	0.002	28,800	28,900	1.1	2.7	2.41	2

[a]Failure occurred in a weld in the gage section of this specimen.

Some idea of the rate of property deterioration with fluence can be obtained by comparing the results for heat 5085 obtained this time on specimens irradiated outside the vessel to a thermal fluence of 1.3×10^{19} neutrons/cm^2 with those obtained previously[9] for specimens removed from the core with a fluence of 1.3×10^{20} neutrons/cm^2. The unknown effects on the properties due to different times at temperature must be recognized; the core specimens for 4800 hr and the vessel specimens for 11,000 hr. The results are compared in Fig. 14.

[9] H. E. McCoy, Jr., An Evaluation of the Molten-Salt Reactor Experiment Hastelloy N Surveillance Specimen — First Group, ORNL-TM-1997 (November 1967).

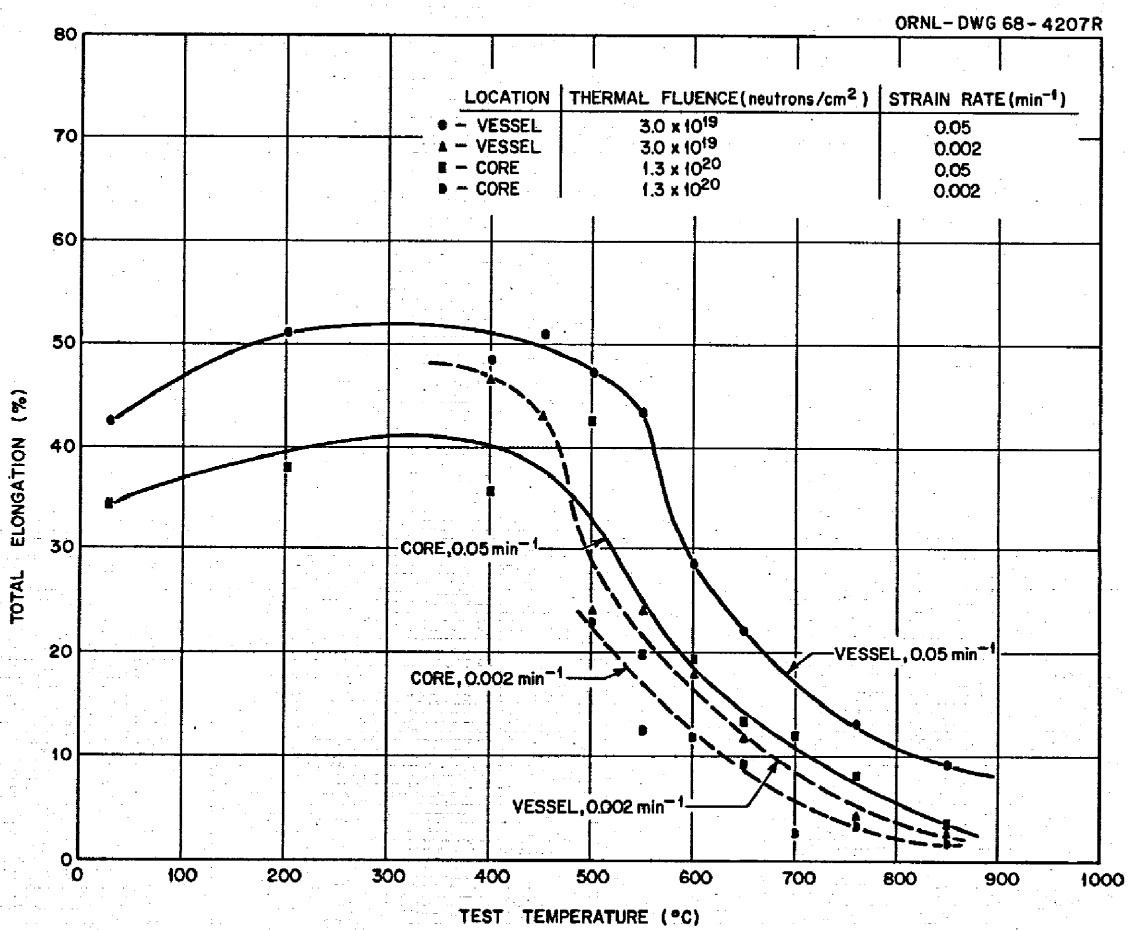

Fig. 14. A Comparison of the Ductility of Surveillance Specimens of Heat 5085 Exposed in the Core and Outside the Core Vessel.

At a strain rate of 0.05 min^{-1}, the fracture strain is decreased appreciably as the thermal fluence increased from 1.3×10^{19} to 1.3×10^{20} neutrons/cm^2. At a slower strain rate of 0.002 min^{-1}, the same trend holds, but the change is much smaller. If this same trend persists to lower strain rates, the fracture strain in creep tests may not be influenced significantly by fluence over the small range studied.

Our previous studies showed that the tensile properties of materials irradiated in the MSRE and those irradiated in the ORR and ETR in a helium environment were similar, the only significant difference being the reduction in fracture strain observed[9] at 25°C. The present results are in good agreement with this conclusion. Our present studies also support previous observations[9] that the yield stress was unaffected by irradiation and that the ultimate tensile stress was reduced about 10% at low temperatures and progressively reduced further above 500°C to a maximum of 30% at 850°C.

The results of several creep-rupture tests on the standard Hastelloy N surveillance specimens from the second group are given in Table 5. The stress-rupture properties are compared in Fig. 15 with

Table 5. Creep-Rupture Properties of Surveillance Specimens of Standard Hastelloy N

Test Number	Specimen Number	Stress Level (psi)	Rupture Life (hr)	Rupture Strain (%)	Minimum Creep Rate (%/hr)
		Heat 5065			
R-320	9030	47,000	23.0	2.10	0.081
R-313	9027	40,000	39.7	2.12	0.034
R-315	9029	32,400	122.3	2.06	0.0078
R-326	9031	27,000	290.2	1.47	0.0035
		Heat 5085			
R-321	9066	47,000	23.2	2.39	0.061
R-312	9063	40,000	61.7	2.28	0.029
R-327	9067	32,400	336.6	2.25	0.0032
R-418	9072	30,000	323.4	2.4	0.0063

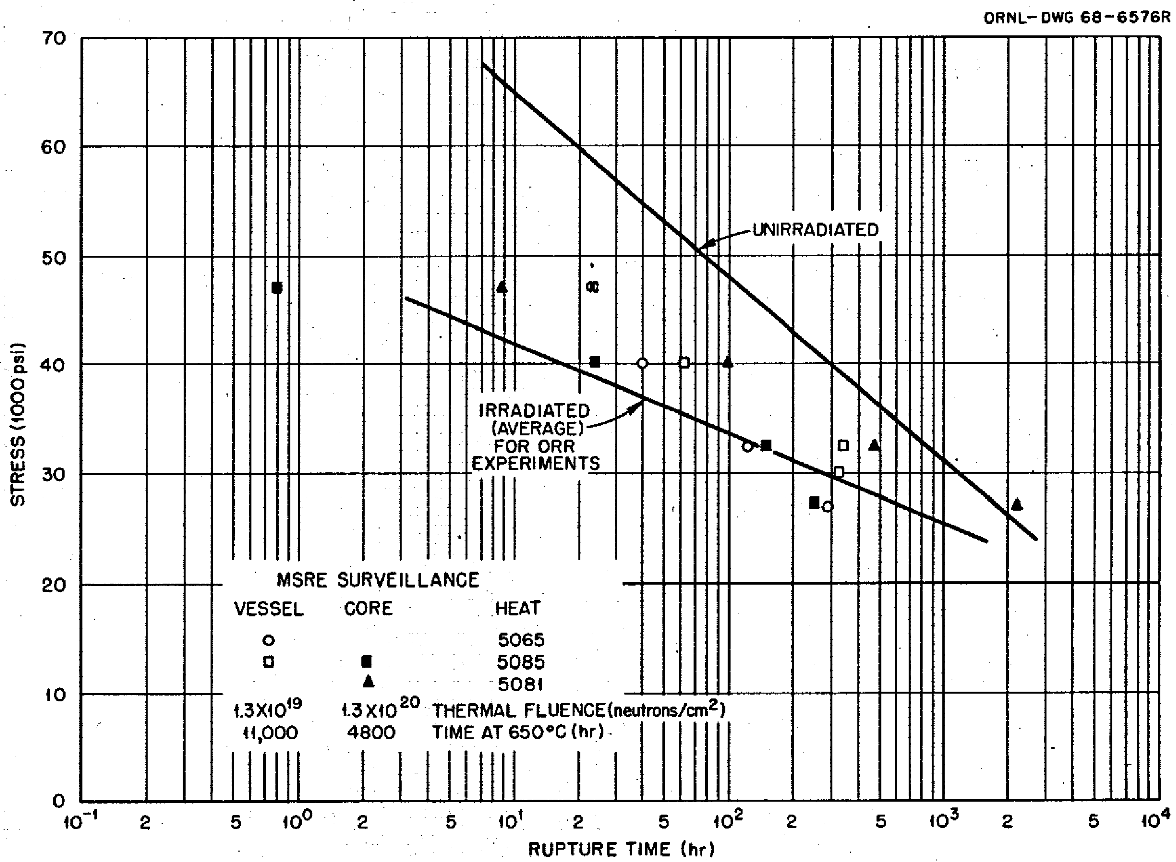

Fig. 15. Postirradiation Creep-Rupture Properties of MSRE Surveillance Specimens at 650°C. Standard Hastelloy N.

those obtained previously on surveillance specimens from the core. The results on heat 5085 show clearly that the rupture life is less for the specimens from the core than for those from outside the vessel. This is probably due to the thermal fluence of the material from the core being higher by a factor of about 10. Heat 5085 seems to have the poorest rupture life and heat 5081 the best; there is no apparent explanation for this behavior. The minimum creep rates for these same materials are compared in Fig. 16. This parameter is not significantly different for the three heats of material involved and is not influenced appreciably by irradiation.

The fracture strains are shown as a function of strain rate in Fig. 17. The scatterband in this figure was determined from results obtained on these same materials irradiated to a thermal fluence of about 2×10^{20} neutrons/cm^2 in the ORR. The fracture strains are significantly

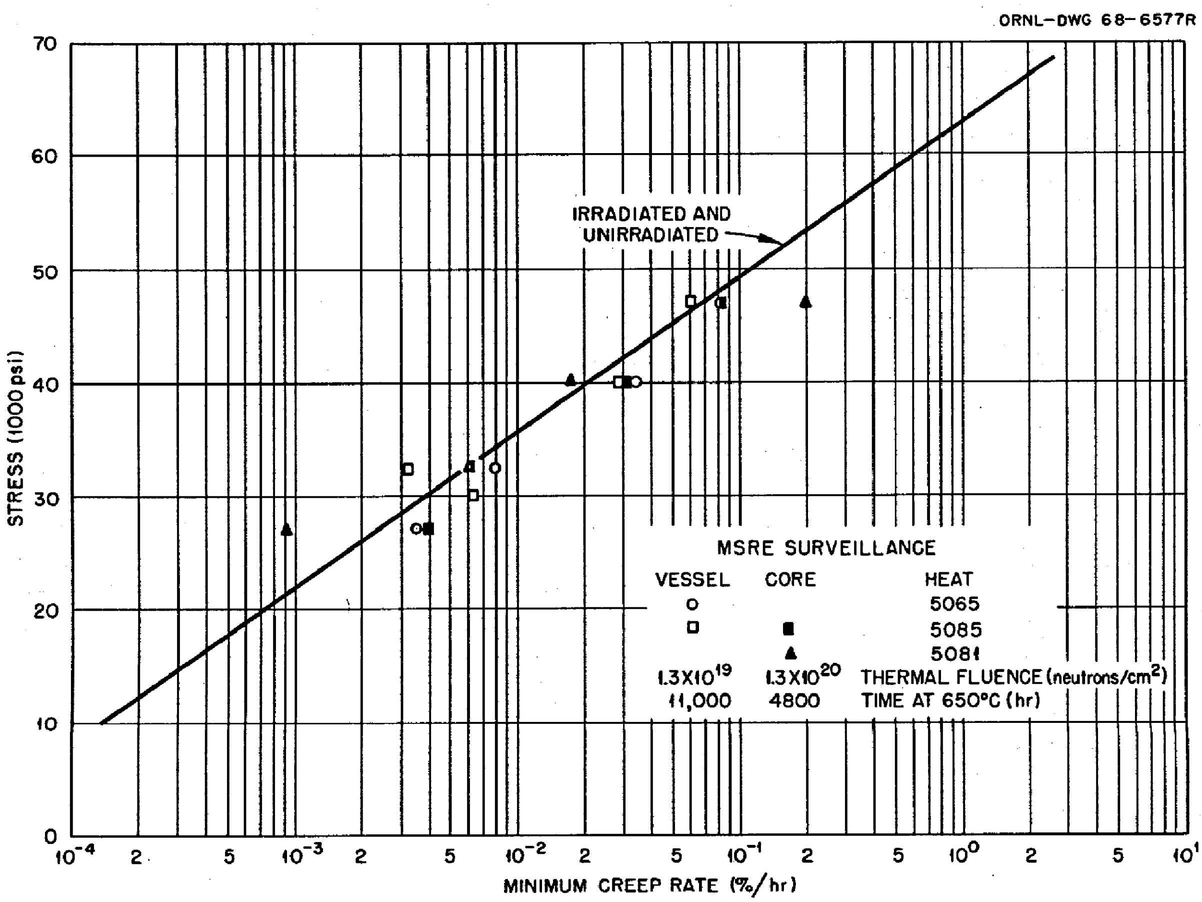

Fig. 16. Variation of Minimum Creep Rate of Hastelloy N MSRE Surveillance Samples in Postirradiation Creep Tests at 650°C.

higher for the specimens irradiated outside the vessel to a thermal fluence of 1.3×10^{19} neutrons/cm^2 when tested at high strain rates (12 to 300%/hr). At lower strain rates most of the fracture strains are in the range of 1.5 to 2.5%. Comparison of the results for the two sets of specimens shows the fracture strains to be slightly lower for the specimens exposed to the higher fluence in the core. These results do not indicate the very pronounced ductility minimum at a strain rate of about 0.1%/hr that is noted for these same materials when irradiated in the ORR. The very long thermal exposures involved may be responsible for this behavior; that is, about 5000 hr in the MSRE compared with only 1000 hr in the ORR. Heat 5081 shows unusually high strains and exhibits the trend of increasing strain with decreasing strain rate.

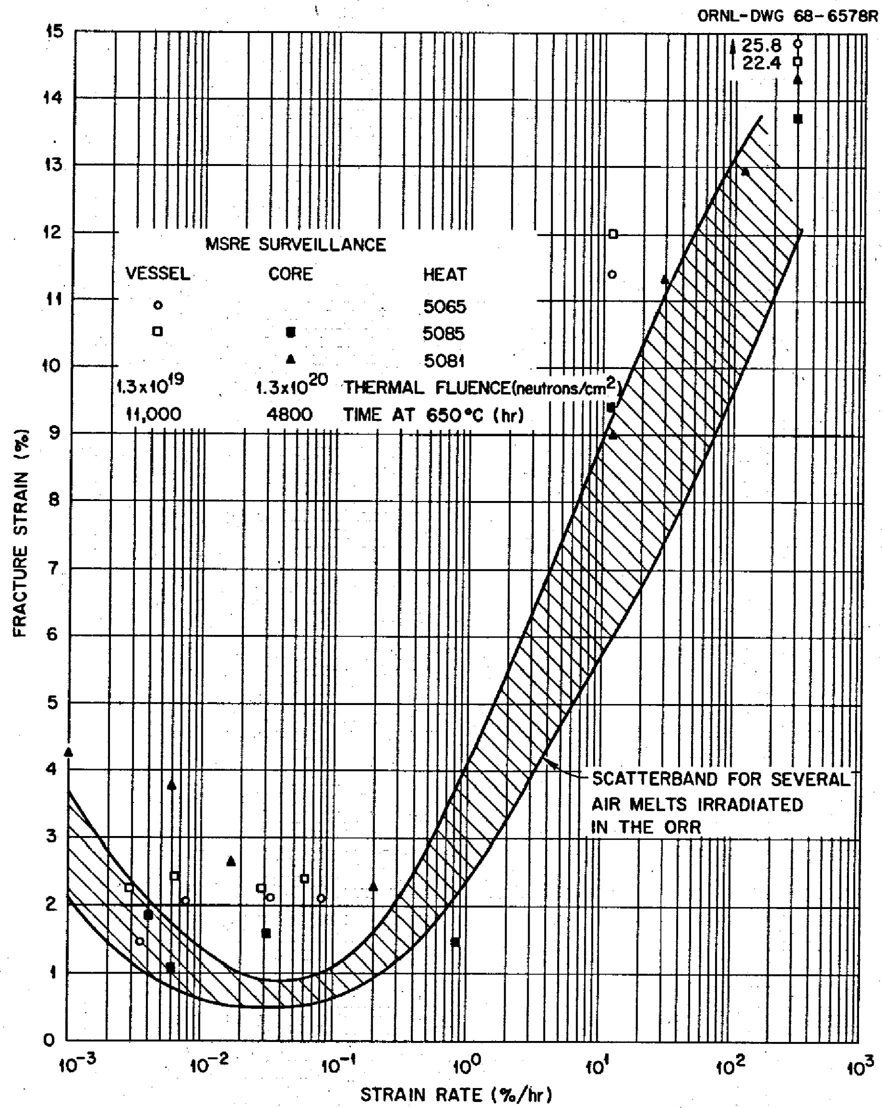

Fig. 17. Variation of Fracture Strain with Strain Rate for MSRE Surveillance Specimen at 650°C. Scatterband is for samples irradiated to a thermal fluence of 3×10^{20} neutrons/cm^2 in the ORR.

Mechanical Property Data — Modified Hastelloy N

Specimens of two modified Hastelloy N alloys were removed from the core surveillance assembly for examination and mechanical testing. Control specimens of these same alloys were exposed to a static vessel of barren salt to duplicate the thermal history of the specimens in the reactor. The tensile properties of the control specimens of heat 21554 (zirconium modified) are given in Table 6; the total strain to fracture is shown in Fig. 18. The behavior is similar to that observed for standard

Table 6. Results of Tensile Tests on MSRE Surveillance Control Specimens — Heat 21554

Specimen Number	Test Temperature (°C)	Strain Rate (min^{-1})	Stress, psi		Elongation, %		Reduction in Area (%)	True Fracture Strain (%)
			Yield	Ultimate	Uniform	Total		
5543	25	0.050	67,700	128,700	42.3	47.0	56.33	83
5544	200	0.050	60,000	115,900	39.9	42.9	59.80	91
5545	400	0.050	54,700	109,200	40.7	44.4	46.82	63
5553	400	0.002	54,200	111,800	45.8	48.3	53.59	77
5546	450	0.050	53,000	107,200	41.3	44.3	54.56	79
5554	450	0.002	55,900	110,500	42.7	48.1	48.26	66
5547	500	0.050	51,400	106,900	42.5	44.8	49.79	69
5555	500	0.002	58,600	111,400	39.9	45.3	43.69	57
5548	550	0.050	58,700	106,900	38.7	43.2	42.73	56
5556	550	0.002	59,800	101,300	26.4	28.0	24.70	28
5549	600	0.050	53,400	102,000	37.0	30.3	31.44	38
5557	600	0.002	56,800	91,000	22.7	25.0	24.18	28
5550	650	0.050	46,400	87,500	27.6	30.4	31.88	38
5558	650	0.002	55,800	75,500	13.3	46.6	63.15	100
5551	760	0.050	43,700	59,000	4.0	8.1	64.27	103
5559	760	0.002	37,900	37,900	1.6	47.4	69.45	119
5552	850	0.050	36,900	37,700	7.5	56.5	69.70	119
5560	850	0.002	22,000	22,000	100.0	46.9	60.94	94

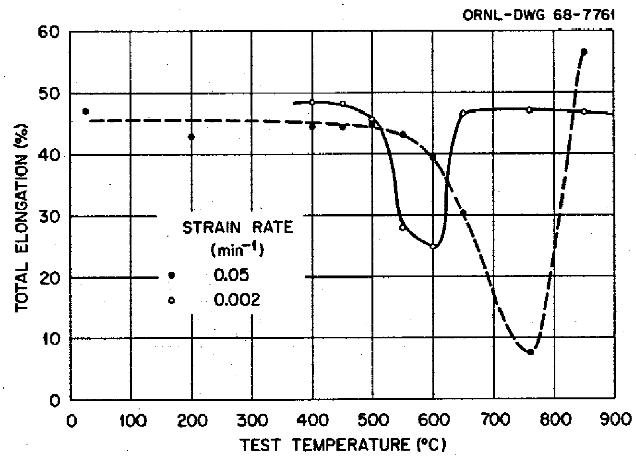

Fig. 18. Variation of the Ductility with Temperature for Control Specimens of Zirconium-Modified Hastelloy N (Heat 21554).

Hastelloy N, but the ductility of the zirconium-modified alloy at 760°C is considerably lower. The strong dependence of fracture strain on strain rate at 760°C is also quite unusual where the strain is higher at the lower strain rate. The properties of this material after irradiation are given in Table 7. The total elongation of the irradiated material is shown in Fig. 19 as a function of test temperatures. The behavior is very similar to that shown in Fig. 14, p. 25, for the standard Hastelloy N exposed under similar conditions; however, the fracture strain at 600 to 700°C is higher for the modified alloy. The ratios of the various properties in the irradiated and unirradiated conditions are shown in Fig. 20. The yield and ultimate strengths were not affected appreciably by irradiation. The ratio for the elongation at fracture drops precipitously above about 600°C for standard Hastelloy N (ref. 10), but the very low elongation observed for the unirradiated zirconium-modified material at 760°C causes the ratio to be very high at this temperature. The behavior of the ratio for the reduction in area is quite normal with the exception of the reduction of this parameter by about 25% at low temperature.

---

[10] H. E. McCoy, Jr., An Evaluation of the Molten-Salt Reactor Experiment Hastelloy N Surveillance Specimen — First Group, ORNL-TM-1997 (November 1967).

Table 7. Results of Tensile Tests on MSRE Surveillance Specimens — Heat 21554

Specimen Number	Test Temperature (°C)	Strain Rate (min^{-1})	Stress, psi		Elongation, %		Reduction in Area (%)	True Fracture Strain (%)
			Yield	Ultimate	Uniform	Total		
9110	25	0.050	64,200	122,100	44.1	47.5	39.08	50
9111	200	0.050	61,000	116,100	43.7	46.0	51.90	73
9112	400	0.050	52,700	109,100	42.5	46.2	34.96	43
9131	400	0.002	64,600	112,600	39.5	45.2	36.26	45
9114	450	0.050	56,000	110,200	39.8	42.3	33.24	40
9132	450	0.002	57,400	107,900	41.8	45.7	33.94	41
9115	500	0.050	56,900	109,900	40.4	43.4	33.48	41
9113	500	0.002	50,500	119,700	43.4	45.6	25.54	29
9116	550	0.050	60,200	107,700	44.5	47.5	36.52	45
9121	550	0.002	43,600	91,700	22.5	23.0	21.15	24
9117	600	0.050	52,700	94,100	31.0	32.0	28.09	33
9122	600	0.002	50,300	80,300	15.7	16.8	18.42	20
9118	650	0.050					25.54	29
9123	650	0.002	48,100	65,600	10.9	11.2	12.39	13
9119	760	0.050	42,400	55,400	6.6	6.8	10.89	12
9124	760	0.002	37,600	37,900	1.7	5.4	4.74	5
9120	850	0.050	34,800	38,600	3.1	6.4	6.27	6
9125	850	0.002	3,800	12,100	5.1	10.4	13.88	15

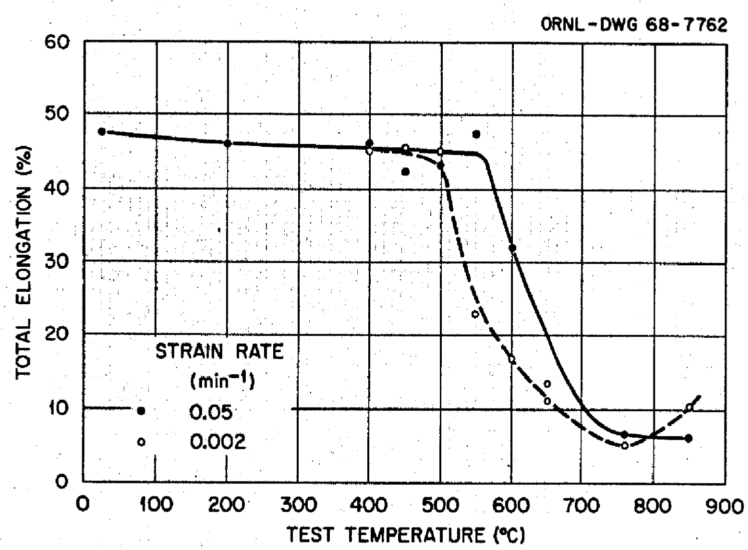

Fig. 19. Variation of the Ductility with Temperature for MSRE Surveillance Specimens of Zirconium-Modified Hastelloy N (Heat 21554). Thermal fluence was 4.1×10^{20} neutrons/cm^2.

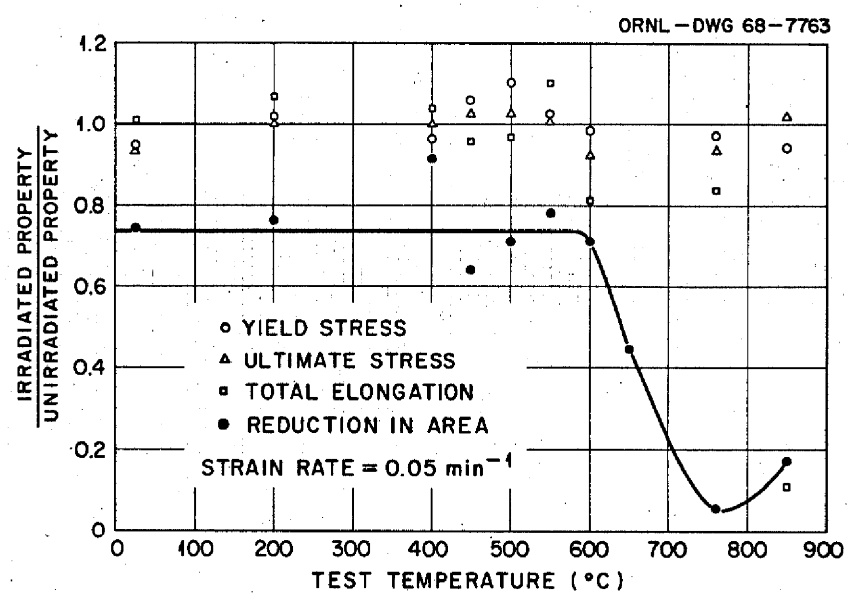

Fig. 20. Comparison of the Tensile Properties of Irradiated and Unirradiated Zirconium-Modified Hastelloy N (Heat 21554). Thermal fluence was 4.1×10^{20} neutrons/cm^2.

The tensile properties of the control specimens of heat 21545 (titanium modified) are given in Table 8. The total elongation is shown in Fig. 21 as a function of the test temperature. The properties are quite similar to those observed for heat 21554 (Fig. 18, p. 31, and Table 6, p. 30). The properties of the surveillance specimens are given in Table 9, and the total elongation at fracture is shown graphically in Fig. 22. The fracture elongations for this material are quite similar to those shown in Fig. 19 for heat 21554. The ratio of the irradiated to the unirradiated property is shown in Fig. 23. Generally the yield strength is increased slightly by irradiation, and the tensile stress is decreased. The elongation at fracture is generally decreased, but decreases precipitously above 600°C. However, the ratio at 760°C is again high due to the extremely low elongation of the unirradiated material. The ratio for the reduction in area is reduced about 30% at low temperatures and decreases rapidly above 600°C.

Several creep-rupture tests have been run on both irradiated and unirradiated specimens of heats 21554 and 21545. The results of tests on these materials are given in Table 10 (annealed 100 hr at 871°C), Table 11 (annealed 100 hr at 871°C and exposed to barren salt for 5500 hr at 650 ± 10°C), and Table 12 (annealed 100 hr at 871°C and exposed to MSRE environment for 5500 hr at 650 ± 10°C). The stress-rupture properties of heat 21554 are compared in Fig. 24 for the various conditions studied. The strength is reduced slightly by the long thermal exposure to barren salt. Exposure to the MSRE environment reduces the rupture life at a given stress by about a factor of 10. The creep rates of heat 21554 are compared in Fig. 25. The minimum creep rate is increased slightly by the 5500 hr soak at about 650°C in the barren salt; the same change is noted for the specimens removed from the MSRE.

The creep-rupture properties of heat 21545 are shown in Fig. 26 for the various conditions studied. Just as noted for the zirconium-modified alloy in Fig. 24, the rupture life of the titanium-modified alloy is reduced slightly by the long soak in the barren salt and the rupture life is reduced by a factor of 10 by exposure to the MSRE environment. The minimum creep rate was not affected significantly by any of the variables investigated, Fig. 27.

Table 8. Results of Tensile Tests on MSRE Surveillance Control Specimens — Heat 21545

Specimen Number	Test Temperature (°C)	Strain Rate (min^{-1})	Stress, psi		Elongation, %		Reduction in Area (%)	True Fracture Strain (%)
			Yield	Ultimate	Uniform	Total		
5531	25	0.050	95,700	127,100	38.1	42.3	61.05	94
5530	200	0.050	49,300	112,800	46.9	50.9	55.45	81
5529	400	0.050	46,000	107,600	46.4	51.1	43.75	58
5521	400	0.002	51,800	111,700	44.5	50.1	59.30	90
5528	450	0.050	50,000	108,700	45.3	48.8	58.14	87
5520	450	0.002	51,100	109,200	45.6	47.7	43.69	57
5527	500	0.050	50,400	104,900	43.7	47.9	51.69	73
5519	500	0.002	47,900	106,900	41.8	45.2	42.06	55
5526	550	0.050	49,500	102,800	42.7	48.0	51.36	72
5518	550	0.002	47,800	93,500	24.9	26.5	31.51	38
5525	600	0.050	43,100	93,300	32.7	34.6	37.67	47
5517	600	0.002	48,000	84,600	23.5	24.6	21.27	24
5524	650	0.050	44,400	84,600	31.0	33.8	28.64	34
5516	650	0.002	45,200	68,500	16.5	40.8	43.84	58
5523	760	0.050	45,900	56,400	3.4	7.3	63.00	99
5515	760	0.002	37,900	37,900	1.3	43.8	63.94	102
5522	850	0.050	33,900	34,200	6.1	53.4	71.83	127
5514	850	0.002	20,100	20,300	0.9	44.0	55.77	82

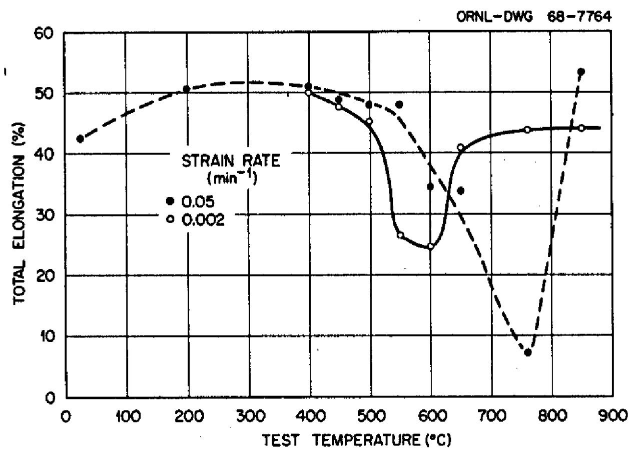

Fig. 21. Variation of the Ductility with Temperature for Control Specimens of Titanium-Modified Hastelloy N (Heat 21545).

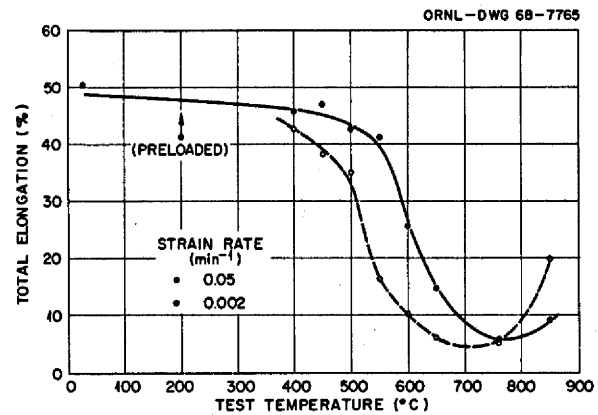

Fig. 22. Variation of the Ductility with Temperature for MSRE Surveillance Specimens of Titanium-Modified Hastelloy N (Heat 21545). Thermal fluence was 4.1×10^{20} neutrons/cm^2.

Table 9. Results of Tensile Tests on MSRE Surveillance Specimens — Heat 21545

Specimen Number	Test Temperature (°C)	Strain Rate (min^{-1})	Stress, psi		Elongation, %		Reduction in Area (%)	True Fracture Strain (%)
			Yield	Ultimate	Uniform	Total		
9083	25	0.050	61,900	145,600	46.3	50.3	45.71	61
9084[a]	200	0.050	80,300	111,200	38.9	41.1	42.53	55
9085	400	0.050	56,100	104,300	42.7	45.7	40.06	51
9105	400	0.002	57,000	107,200	37.5	42.6	47.58	65
9086	450	0.050	54,200	104,300	44.5	47.0	37.54	47
9106	450	0.002	57,000	102,700	35.8	38.2	32.10	39
9088	500	0.050	54,700	102,700	41.1	42.7	36.78	46
9089	500	0.002	53,000	86,700	32.2	35.2	29.88	35
9090	550	0.050	46,900	95,800	38.7	41.2	40.12	51
9094	550	0.002	57,100	91,600	15.3	16.5	23.35	27
9091	600	0.050	44,500	83,600	25.2	25.7	26.93	31
9096	600	0.002	46,900	66,200	9.6	10.4	16.83	18
9092	650	0.050	45,200	73,700	13.4	14.6	12.79	14
9097	650	0.002	48,900	58,900	5.4	6.2	4.74	5
9093	760	0.050	39,000	46,800	5.4	5.8	3.98	4
9098	760	0.002	31,200	31,200	1.3	5.7	5.54	6
9095	850	0.050	33,500	33,600	1.7	9.2	12.39	13
9104	850	0.002	8,100	10,600	1.1	20.2	19.07	21

[a]Test preloaded; therefore measured yield stress higher than normal and elongation lower.

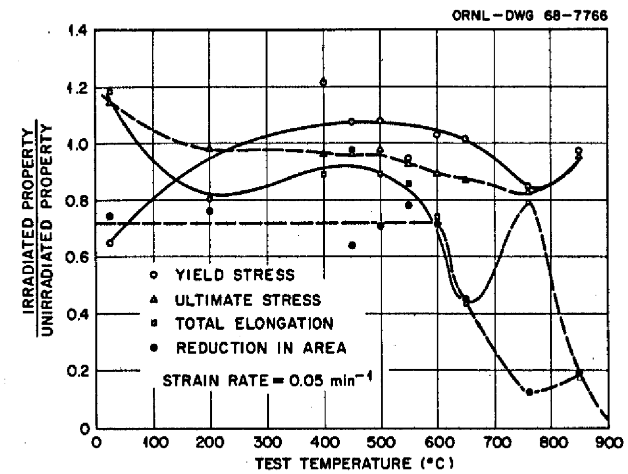

Fig. 23. Comparison of the Tensile Properties of Irradiated and Unirradiated Titanium-Modified Hastelloy N (Heat 21545). Thermal fluence was 4.1×10^{20} neutrons/cm^2.

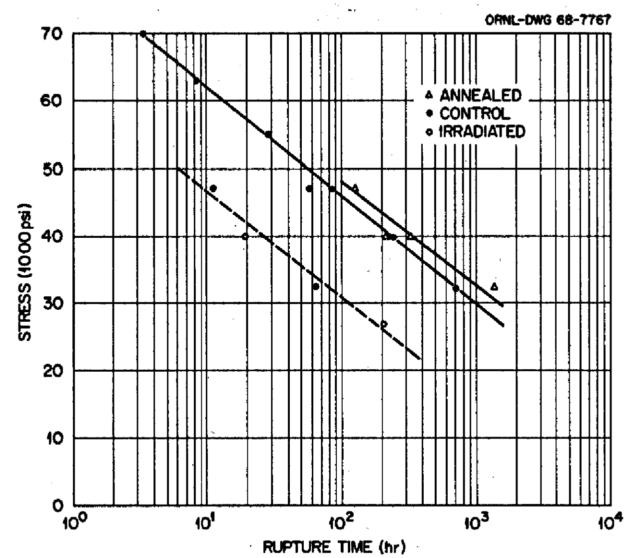

Fig. 24. Creep-Rupture Properties of Zirconium-Modified Hastelloy N (Heat 21554) at 650°C in Several Conditions; Annealed at 871°C (see p. 7); Annealed at 871°C and Aged for 5500 hr at 650°C in Static Fluoride Salt; and Irradiated to a Thermal Fluence of 4.1×10^{20} neutrons/cm^2.

Table 10. Creep-Rupture Properties of Heats 21545 and 21554 at 650°C After Annealing 100 hr at 871°C

Test Number	Specimen Number	Stress (psi)	Rupture Life (hr)	Rupture Strain (%)	Reduction in Area (%)	Minimum Creep Rate (%/hr)	True Fracture Strain (%)
				Heat 21554			
5862	2435	47,000	128.3	63.0	50.6	0.203	71
5857	2434	40,000	324.2	35.5	51.9	0.056	73
5858	2491	40,000	226.3	60.8	50.9	0.128	71
6168	2433	32,400	1390.9	55.1	42.4	0.0176	55
				Heat 21545			
5409	1771	55,000	20.1	52.5	47.3	1.37	64
5564	1822	40,000	248.1	34.4	20.5	0.0688	23
5580	1773	40,000	242.6	59.4	56.6	0.120	84
5449	1768	30,000	1171.5	56.7	51.5	0.0174	72

Table 11. Creep-Rupture Properties of MSRE Surveillance Control Specimens at 650°C

Test Number	Specimen Number	Stress (psi)	Rupture Life (hr)	Rupture Strain (%)	Reduction in Area (%)	Minimum Creep Rate (%/hr)	True Fracture Strain (%)
				Heat 21554			
6399	5535	70,000	3.3	60.6	48.3	8.375	67
6398	5536	63,000	8.3	50.0	50.1	3.20	70
6397	5537	55,000	28.2	55.8	45.0	1.01	60
6389	5538	47,000	58.1	38.3	58.3	0.365	88
6425	5540	47,000	84.1	75.1	56.0	0.363	82
6390	5539	40,000	228.7	69.5	56.6	0.120	84
6426	5541	40,000	244.0	63.1	49.6	0.113	69
6427	5542	32,400	709.8	56.1	49.7	0.032	69
				Heat 21545			
6384	5508	70,000	1.9	39.2	30.6		36
6385	5509	63,000	5.5	46.1	32.7	4.50	40
6386	5510	55,000	15.7	47.4	34.3	2.50	42
6387	5511	47,000	50.8	43.9	44.4	0.50	59
6388	5512	40,000	177.2	55.3	45.1	0.165	60
6428	5513	32,400	438.8	40.1	49.8	0.0398	69

Table 12. Creep-Rupture Properties of Surveillance Specimens of Modified Hastelloy N at 650°C

Test Number	Specimen Number	Stress Level (psi)	Rupture Life (hr)	Rupture Strain (%)	Minimum Creep Rate (%/hr)
		Heat 21554			
R-316	9127	47,000	11.1	4.57	0.343
R-311	9126	40,000	19.3	3.99	0.138
R-318	9128	32,400	65.4	2.36	0.013
R-322	9129	27,000	204.9	3.45	0.0088
		Heat 21545			
R-317	9100	47,000	2.8	1.59	0.455
R-314	9099	40,000	13.1	2.68	0.085
R-319	9102	32,400	51.1	3.39	0.0180
R-323	9103	27,000	124.1	3.69	0.0089

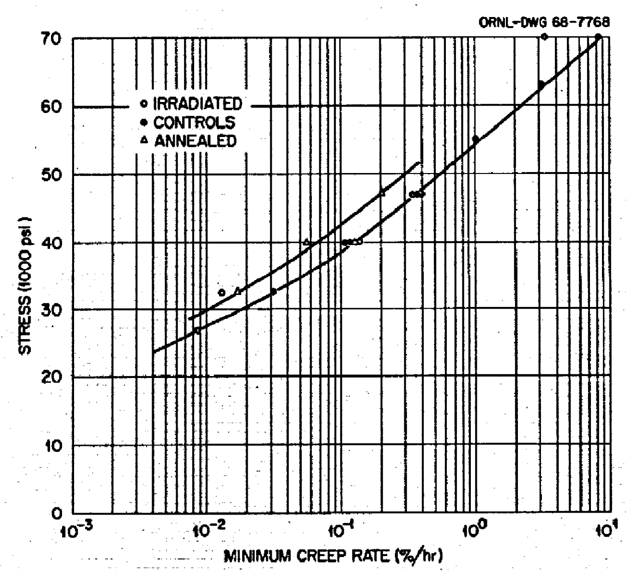

Fig. 25. Variation of the Minimum Creep Rate with Stress for Zirconium-Modified Hastelloy N (Heat 21554) at 650°C. Tested after annealing at 871°C (see p. 7), annealing followed by 5500 hr at 650°C in static fluoride salt, and irradiated to a thermal fluence of 4.1×10^{20} neutrons/cm^2.

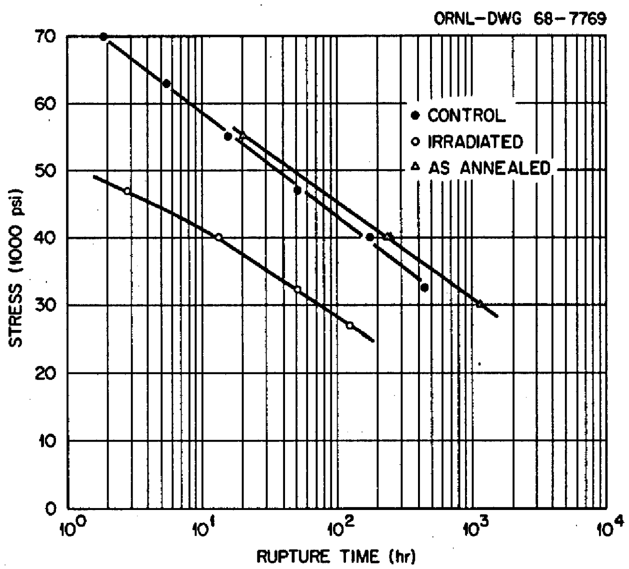

Fig. 26. Creep-Rupture Properties of Titanium-Modified Hastelloy N (Heat 21545) at 650°C in Several Conditions: Annealed at 871°C (see p. 7), Annealed at 871°C and Aged for 5500 hr at 650°C in Static Fluoride Salt, and Irradiated to a Thermal Fluence of 4.1×10^{20} neutrons/cm^2.

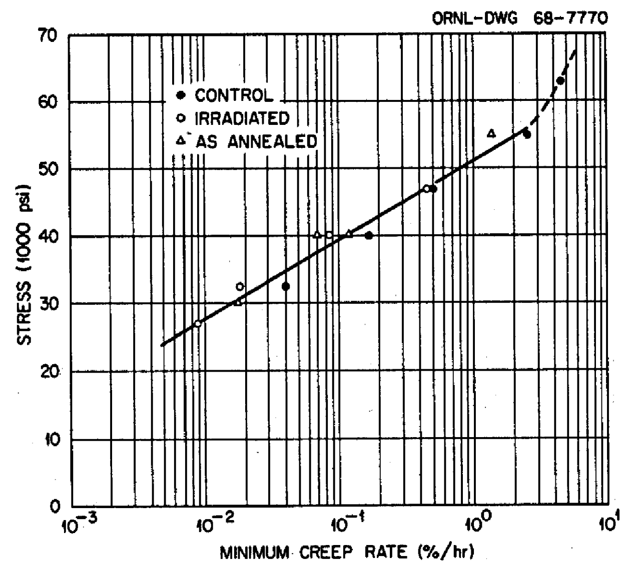

Fig. 27. Variation of the Minimum Creep Rate with Stress for Titanium-Modified Hastelloy N (Heat 21545) at 650°C. Tested after annealing at 871°C (see p. 7), annealing followed by 5500 hr at 650°C in static fluoride salt, and irradiated to a thermal fluence of 4.1×10^{20} neutrons/cm^2.

The fracture strains of these materials in the unirradiated state under creep conditions are excellent, ranging from 30 to 60% (Tables 10 and 11). However, the fracture strains after irradiation are appreciably less ranging from 1.5 to 4.5% (Table 12). These strains are generally higher than those obtained from standard Hastelloy N (Fig. 17, p. 29).

Metallographic Examination of Mechanical Property Specimens

Several of the fractured test specimens were examined metallographically. Typical micrographs from a specimen of heat 5065 exposed to the cell environment for 11,000 hr and tested at room temperature are shown in Fig. 28. Figure 28(a) shows the fracture region and demonstrates the mixed intergranular-transgranular nature of the fracture. The edge of the gage section is shown in Fig. 28(b). There is very little edge-cracking or other indications of deleterious reactions with the MSRE cell environment. Large quantities of fine precipitate that formed during the long thermal history are also obvious. A higher magnification photomicrograph made near the surface is shown in Fig. 28(c). Significant features are the limited surface reaction and the copious quantities of fine precipitates.

Photomicrographs of a specimen from heat 5065 tested at 650°C are shown in Fig. 29. The fracture shown in Fig. 29(a) is completely intergranular and typical of materials exhibiting low fracture strains.

The microstructure of a specimen from heat 5065 that was tested in creep at 650°C and 27,000 psi is illustrated in Fig. 30. Figure 30(a) shows that the fracture is entirely intergranular with some cracking near the fracture. Figure 30(b) and (c) shows the thin reaction layer at the surface and the large amount of fine precipitate that formed.

Several photomicrographs of the specimen of heat 5085 tested at 25°C are shown in Fig. 31. The gage portion of this specimen contained a weld and the failure occurred in this region [Fig. 31(a)]. There is a very thin region near the surface that shows some modification of microstructure [Fig. 31(b) and (c)]. This layer is quite similar in

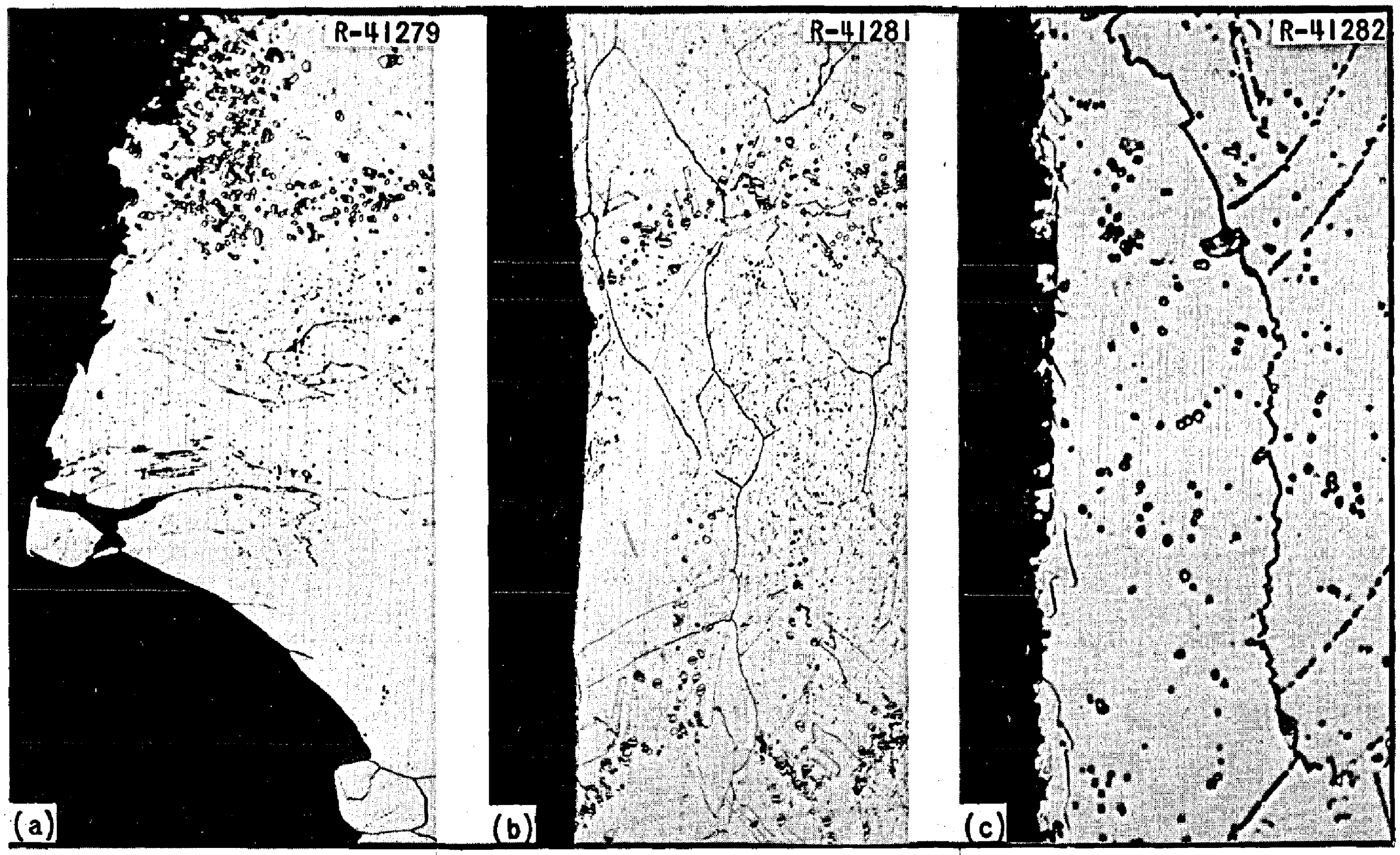

Fig. 28. Photomicrographs of a Hastelloy N Surveillance Sample (Heat 5065) Tested at 25°C at a Strain Rate of 0.05 min^{-1}. Exposed outside the core for 11,000 hr at 650°C to a thermal fluence of 1.3×10^{19} neutrons/cm^2. Etchant: Aqua regia. (a) Fracture — note the mixed transgranular and intergranular fracture. 100×. (b) Edge of sample about 1/2 in. from fracture. Note the fractured precipitates. 100×. (c) Edge of sample showing shallow surface oxidation and extensive precipitation. 500×.

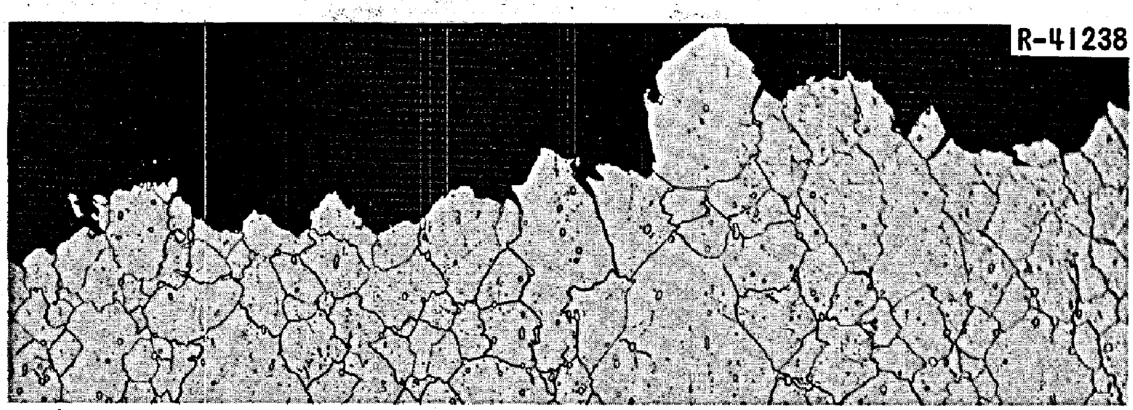

Fig. 29. Photomicrograph of the Fracture of a Standard Hastelloy N Surveillance Sample (Heat 5065) Tested at 650°C at a Strain Rate of 0.002 min^{-1}. Exposed outside the core for 11,000 hr at 650°C to a thermal fluence of 1.3×10^{19} neutrons/cm^2. 100×. Etchant: Aqua regia.

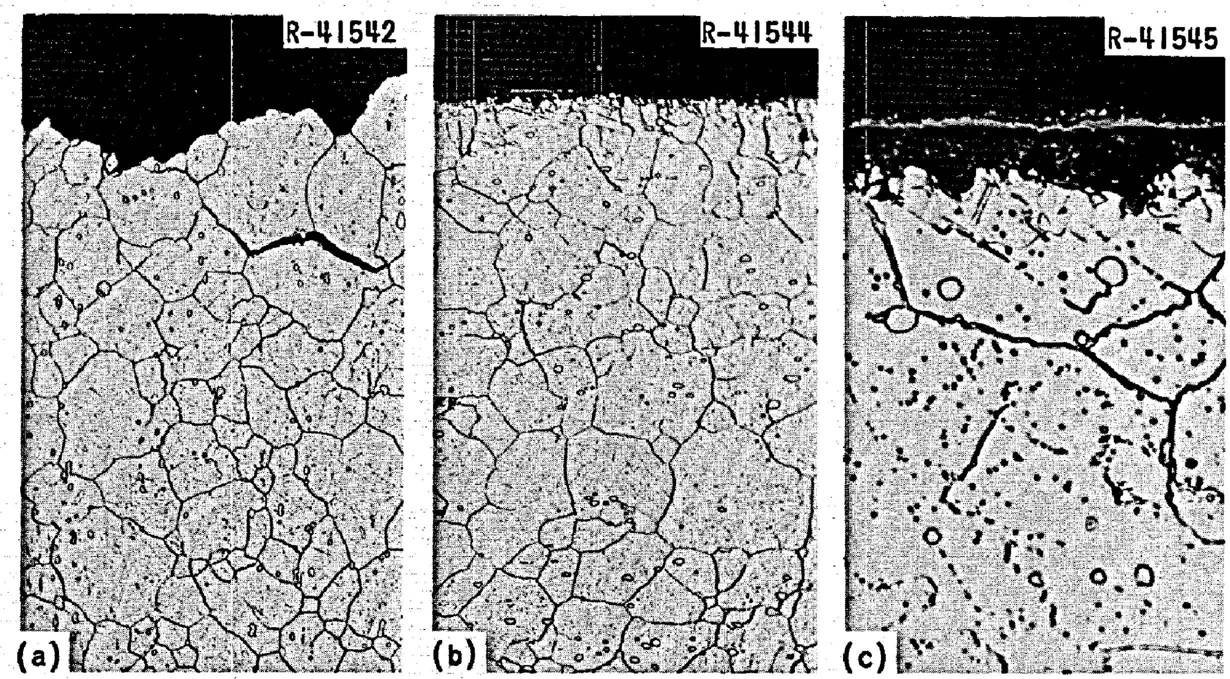

Fig. 30. Photomicrographs of a Standard Hastelloy N Surveillance Sample (Heat 5065) Tested at 650°C and 27,000 psi. Failed in 290 hr after straining 1.47%. Prior to testing, the sample was exposed outside the MSRE core for 11,000 hr at 650°C to a thermal fluence of 1.3×10^{19} neutrons/cm^2. Etchant: Aqua regia. (a) Fracture — note the predominately intergranular fracture. 100×. (b) Edge of sample about 1/2 in. from fracture. 100×. (c) Edge of sample showing shallow oxidation and extensive precipitation. 500×.

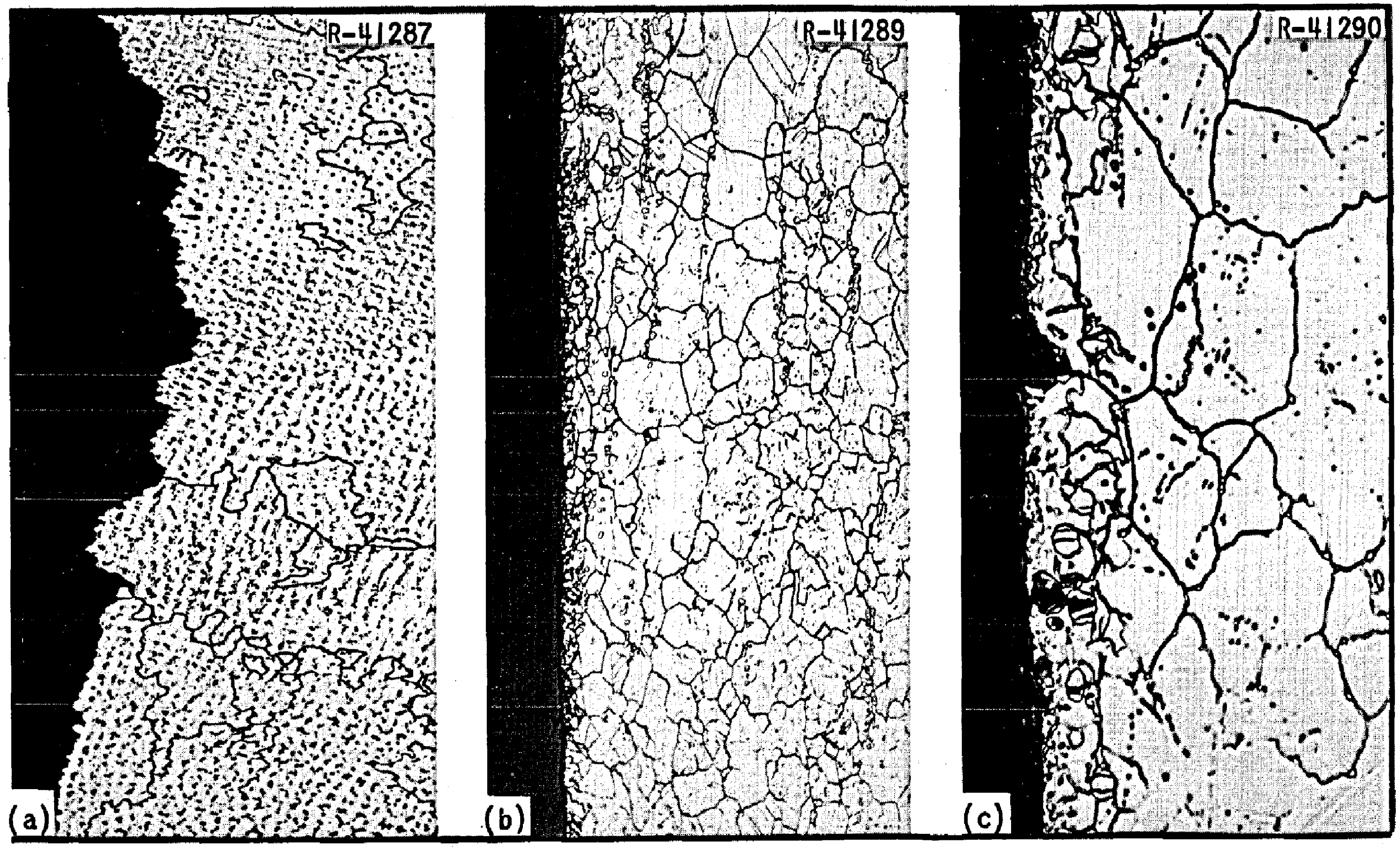

Fig. 31. Photomicrographs of a Standard Hastelloy N Surveillance Sample (Heat 5085) Tested at 25°C at a Strain Rate of 0.05 min^{-1}. Exposed outside the core for 11,000 hr at 650°C to a thermal fluence of 1.3×10^{19} $neutrons/cm^2$. Etchant: Aqua regia. (a) Fracture in a weld that was made in the gage length in fabricating the rod. 100×. (b) Edge of sample about 1/2 in. from fracture. 100×. (c) Edge of sample showing shallow surface reaction, grain boundary precipitates, and fractured precipitates. 500×.

appearance to that noted previously[11] for this material when exposed to the core environment. However, this layer seems to have only minor effects on the deformation as evidenced by the very limited surface cracking shown in Fig. 31(c).

The fracture of a specimen from heat 5085 that was tested at 650°C is shown in Fig. 32. The fracture is completely intergranular and shows little evidence of plastic deformation. A comparison of Figs. 32 and 31(b) gives an indication of the wide variation in the grain size of this material.

---

[11]H. E. McCoy, Jr., An Evaluation of the Molten-Salt Reactor Experiment Hastelloy N Surveillance Specimen — First Group, ORNL-TM-1997 (November 1967).

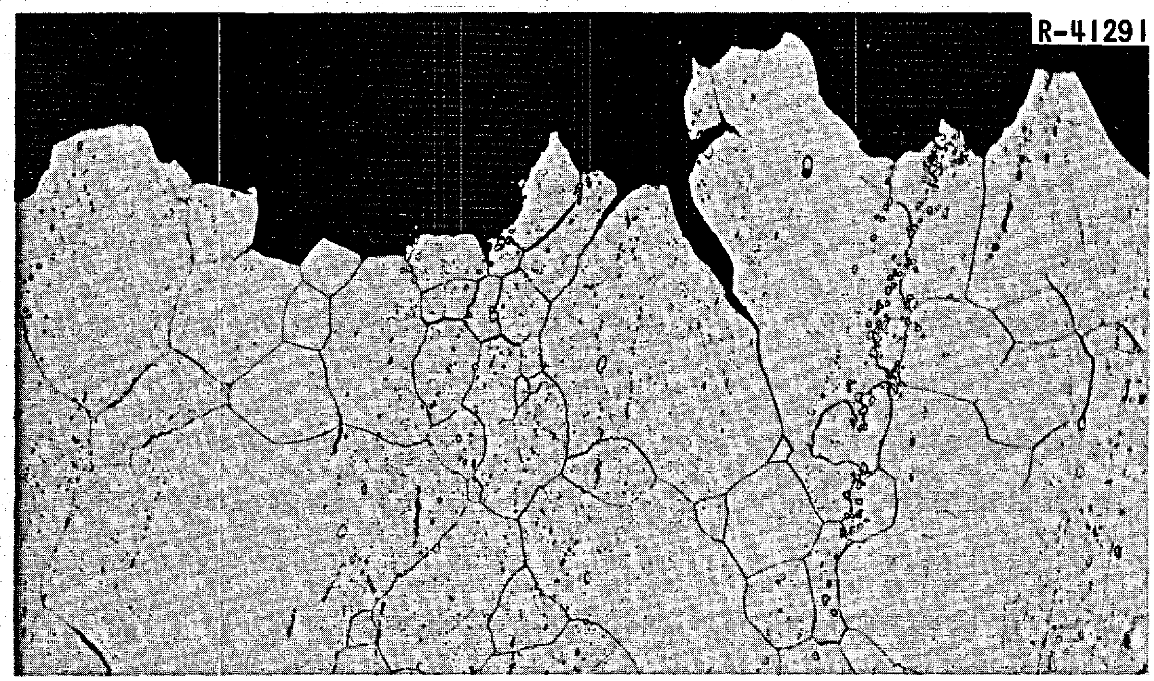

Fig. 32. Photomicrograph of the Fracture of a Standard Hastelloy N Surveillance Sample (Heat 5085) Tested at 650°C at a Strain Rate of 0.002 min^{-1}. Exposed outside the core for 11,000 hr at 650°C to a thermal fluence of 1.3×10^{19} $neutrons/cm^2$. 100×. Etchant: Aqua regia.

Photomicrographs of a specimen of heat 5085 that was tested in creep at 650°C are shown in Fig. 33. The fracture is entirely intergranular with a few cracks near the fracture. The thin reaction layer near the surface is apparent in Fig. 33(b) and (c).

Both the control and the irradiated specimens from heats 21554 and 21545 were exposed to salt for 5500 hr. The microstructures of these alloys before stressing were shown in Figs. 5 and 6, pp. 14 and 15. The microstructure of a specimen from heat 21554 that was tested at 25°C is shown in Fig. 34. The fracture was predominately transgranular. There was a layer near the surface of the specimen that showed extensive intergranular cracking [Fig. 34(b) and (c)]. A typical photomicrograph of the control sample is shown in Fig. 35. The fracture is a typical ductile shear type and there is no appreciable edge cracking.

The microstructure of a specimen of heat 21554 tested at 650°C is illustrated in Fig. 36. The fracture is intergranular and relatively brittle in appearance [Fig. 36(a)]. The edge cracking is quite extensive at this temperature also. The fracture of the control specimen (Fig. 37) is mixed intergranular-transgranular. There is some edge cracking, but not at the frequency noted for the irradiated sample [Fig. 36(b)].

At a test temperature of 850°C, the fracture strain for heat 21554 after irradiation was higher than at 650°C. The microstructures shown in Fig. 38 for the specimen tested at 850°C support this observation. The fracture is entirely intergranular with extensive intergranular cracking throughout the sample. The edge cracking is not quite as severe at this temperature [Fig. 38(b) and (c)]. The fracture of the control sample is shown in Fig. 39. The original grain structure has been fragmented completely because of the very high mobility of the grain boundaries at this temperature.

The microstructural features of heat 21545 were quite similar to those for heat 21554. Typical photomicrographs for heat 21545 are shown in Figs. 40 through 45 for tensile test temperatures of 25, 650, and 850°C. Significant features are the shear fracture at 25°C in the irradiated and unirradiated conditions, the extensive edge cracking in the

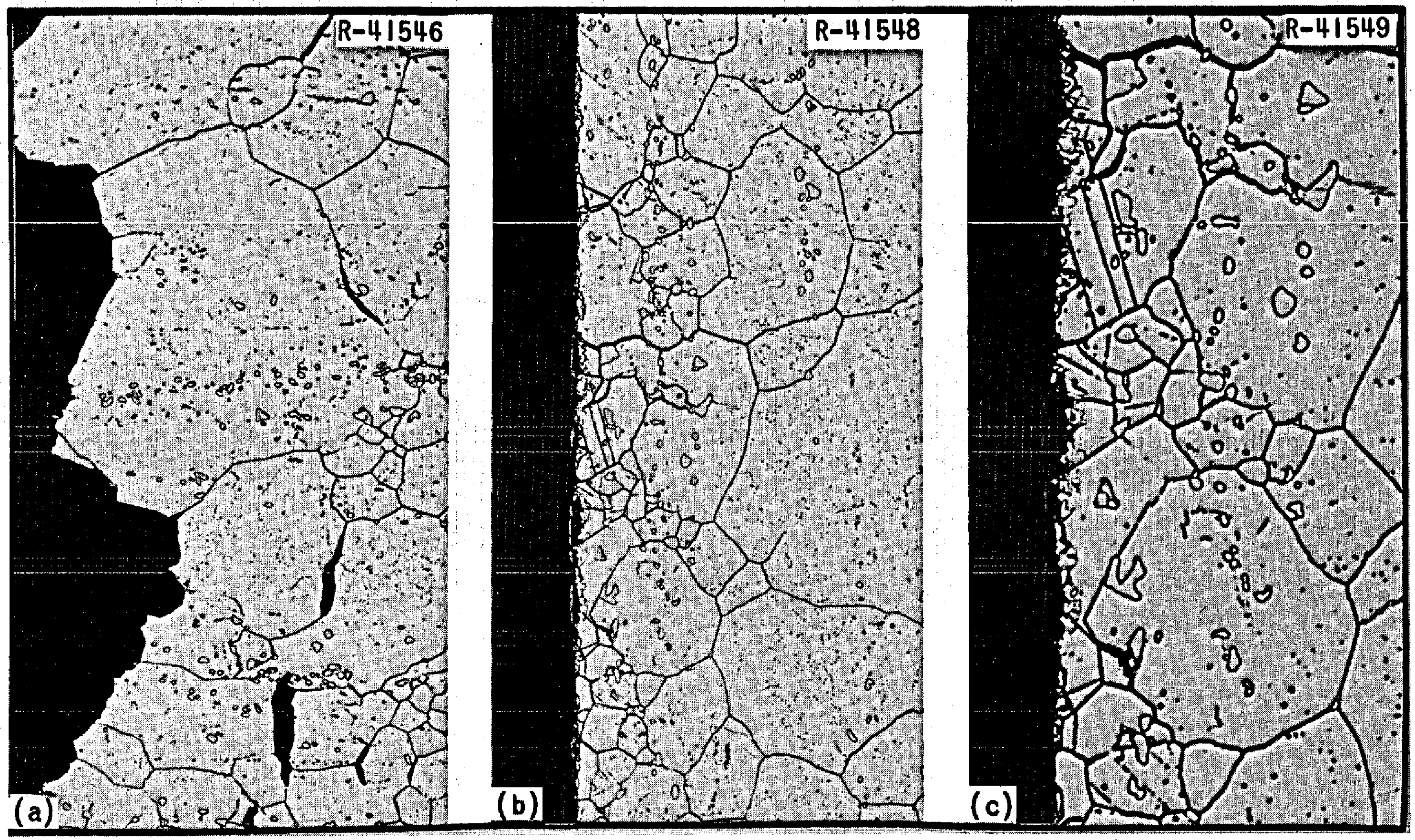

Fig. 33. Photomicrographs of a Standard Hastelloy N Surveillance Sample (Heat 5085) Tested at 650°C and 30,000 psi. Failed in 323.4 hr after straining 2.4%. Prior to testing, the sample was exposed outside the MSRE core for 11,000 hr at 650°C to a thermal fluence of 1.3×10^{19} neutrons/cm^2. Etchant: Aqua regia. (a) Fracture. 100×. (b) Edge of sample about 1/2 in. from fracture. 100×. (c) Edge of sample showing shallow surface oxidation and extensive precipitation. 500×.

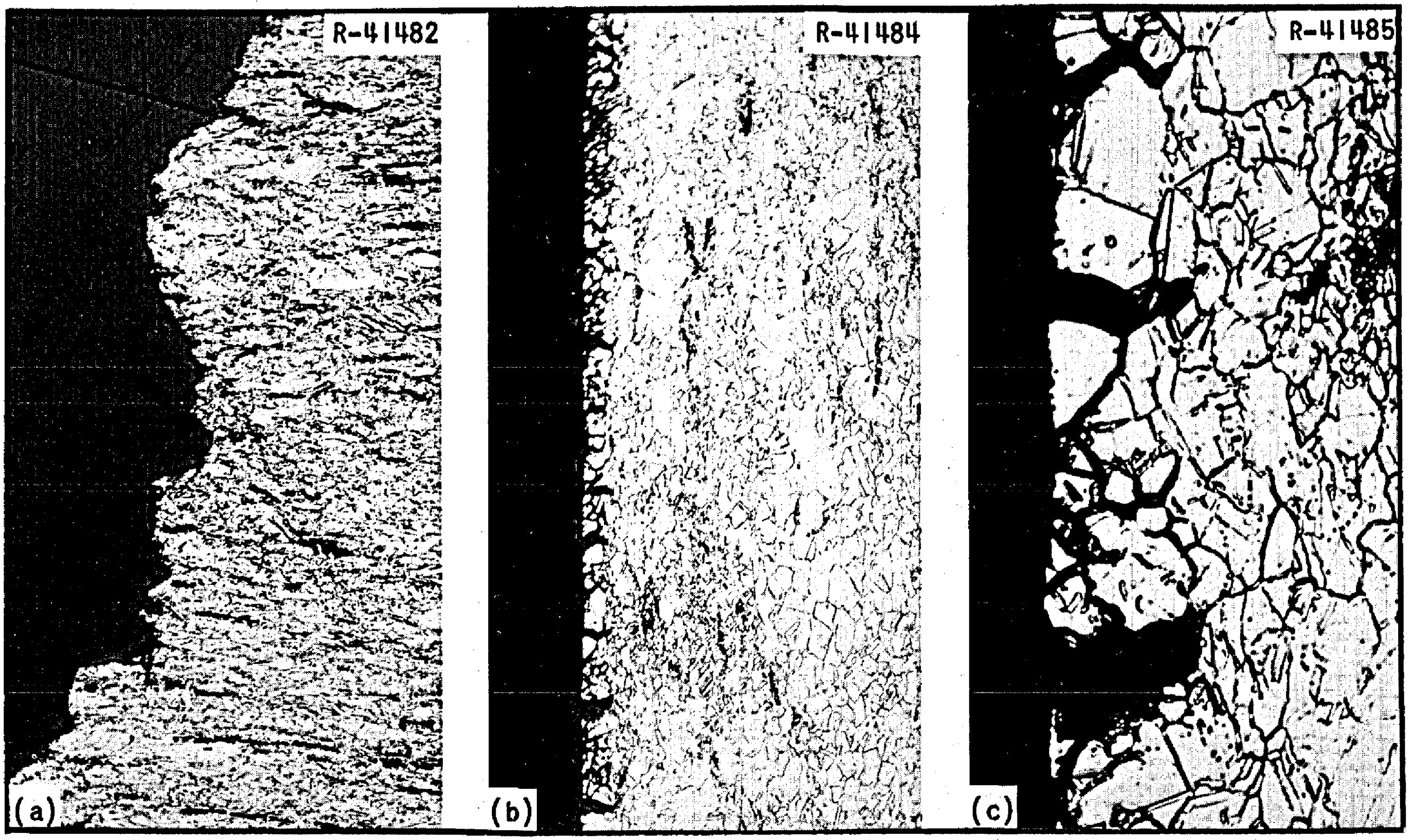

Fig. 34. Photomicrographs of a Zirconium-Modified Hastelloy N Surveillance Sample (Heat 21554) Tested at 25°C at a Strain Rate of 0.05 min^{-1}. Exposed in the MSRE core for 5500 hr at 650°C to a thermal fluence of 4.1×10^{20} $neutrons/cm^2$. Etchant: Aqua regia. (a) Fracture. 100×. (b) Edge of sample about 1/2 in. from fracture. 100×. (c) Edge of sample showing edge cracking. 500×.

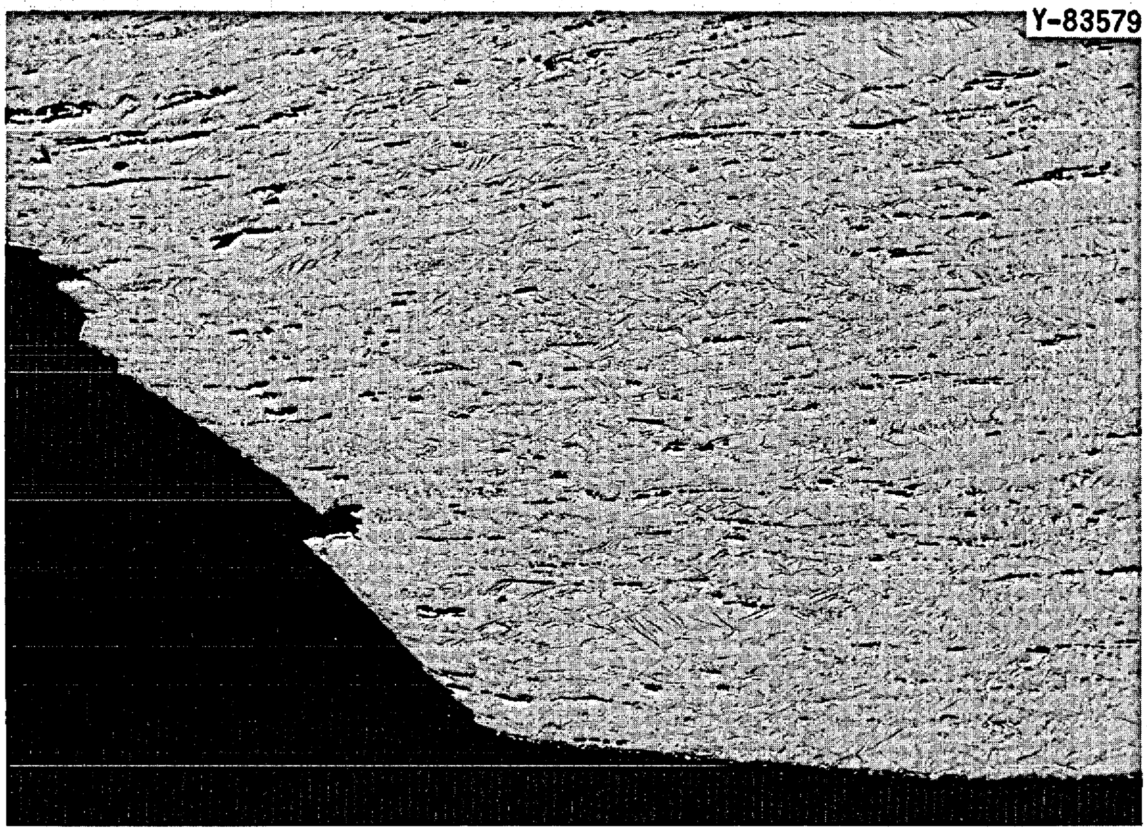

Fig. 35. Photomicrograph of the Fracture of a Zirconium-Modified Hastelloy N Sample (Heat 21554) Tested at 25°C at a Strain Rate of 0.05 min^{-1}. Exposed to a static fluoride salt for 5500 hr at 650°C before testing. Note the shear fracture and the absence of edge cracking. 100×. Etchant: Glyceria regia.

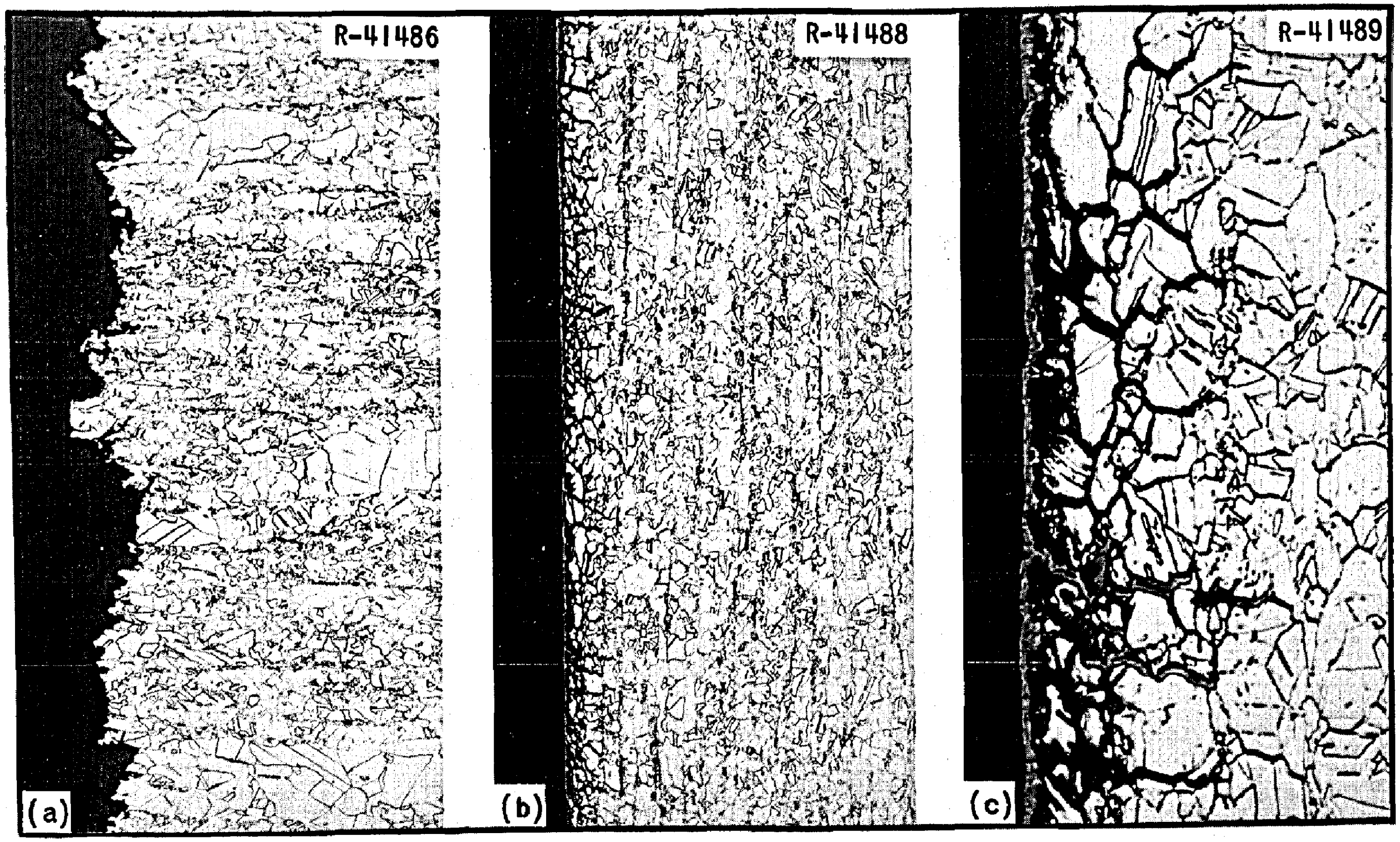

Fig. 36. Photomicrographs of a Zirconium-Modified Hastelloy N Surveillance Sample (Heat 21554) Tested at 650°C at a Strain Rate of 0.002 min^{-1}. Exposed in the MSRE core for 5500 hr at 650°C to a thermal fluence of 4.1×10^{20} $neutrons/cm^2$. Etchant: Aqua regia. (a) Fracture. 100×. (b) Edge of sample about 1/2 in. from fracture. 100×. (c) Edge of sample showing edge cracking. Oxide formed during the tensile test. 500×.

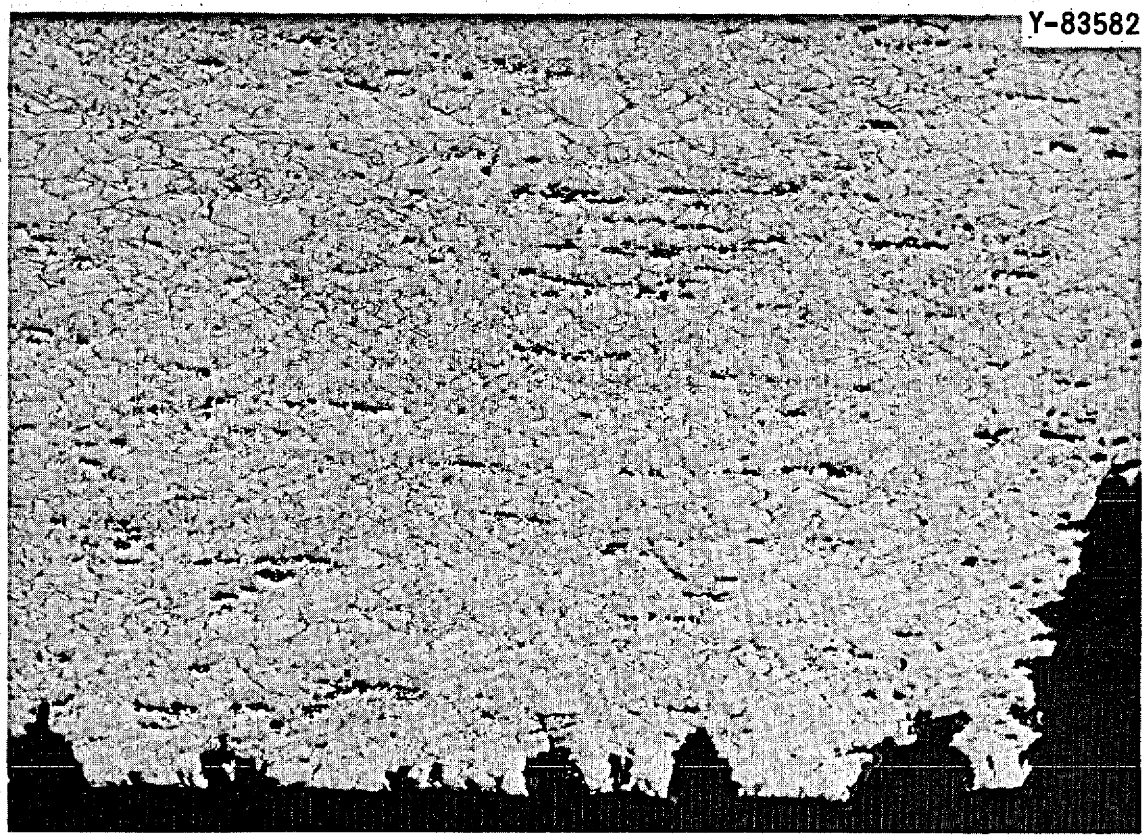

Fig. 37. Photomicrograph Showing a Portion of the Fracture of a Zirconium-Modified Hastelloy N Sample (Heat 21554) Tested at 650°C at a Strain Rate of 0.002 min^{-1}. Exposed to static fluoride salt for 5500 hr at 650°C before testing. 100×. Etchant: Glyceria regia.

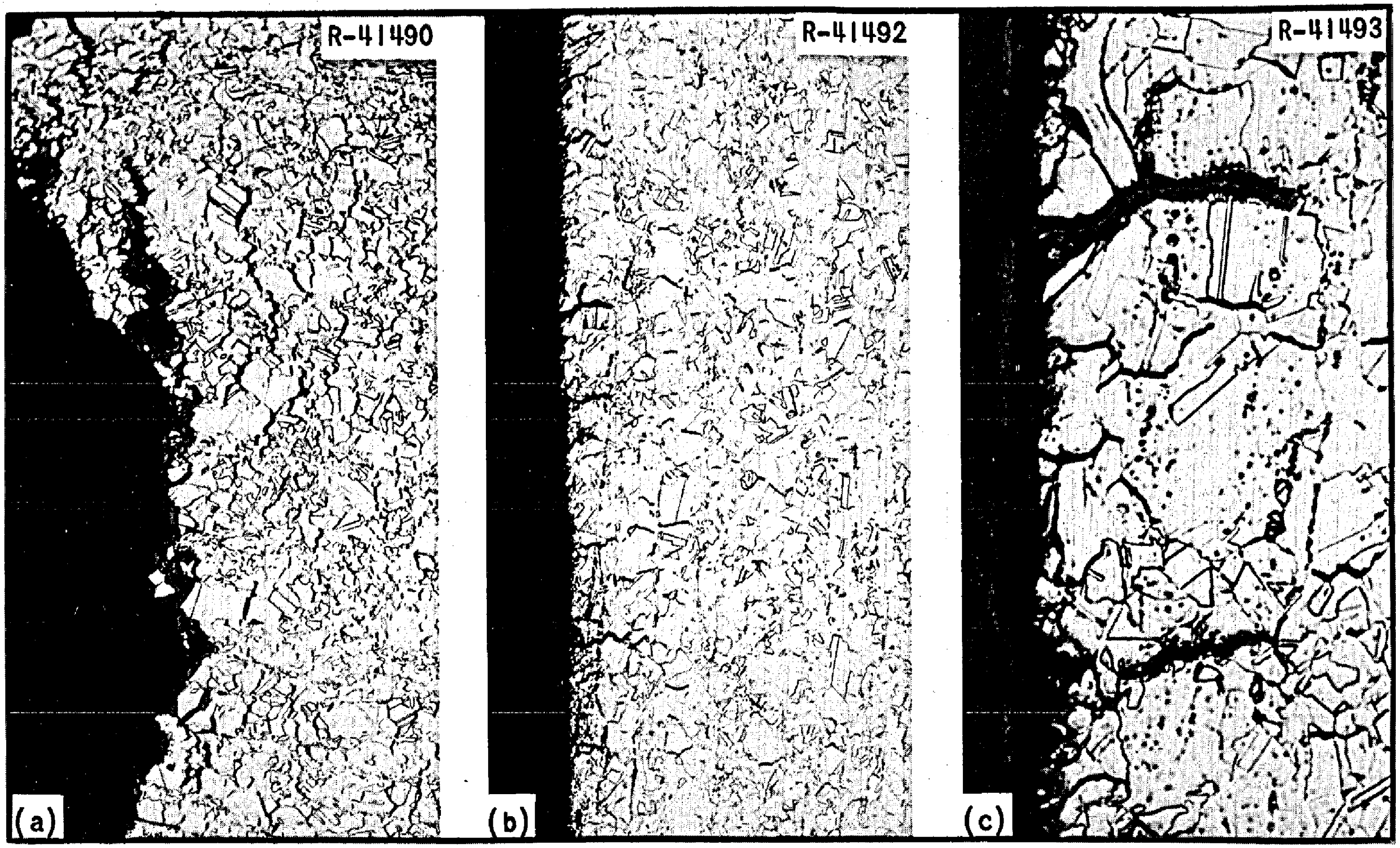

Fig. 38. Photomicrographs of a Zirconium-Modified Hastelloy N Surveillance Sample (Heat 21554) Tested at 850°C at a Strain Rate of 0.002 min^{-1}. Exposed in the MSRE core for 5500 hr at 650°C to a thermal fluence of 4.1×10^{20} $neutrons/cm^2$. Etchant: Aqua regia. (a) Fracture. 100×. (b) Edge of sample about 1/2 in. from fracture. 100×. (c) Edge of sample showing edge cracking. Oxide formed during the tensile test. 500×.

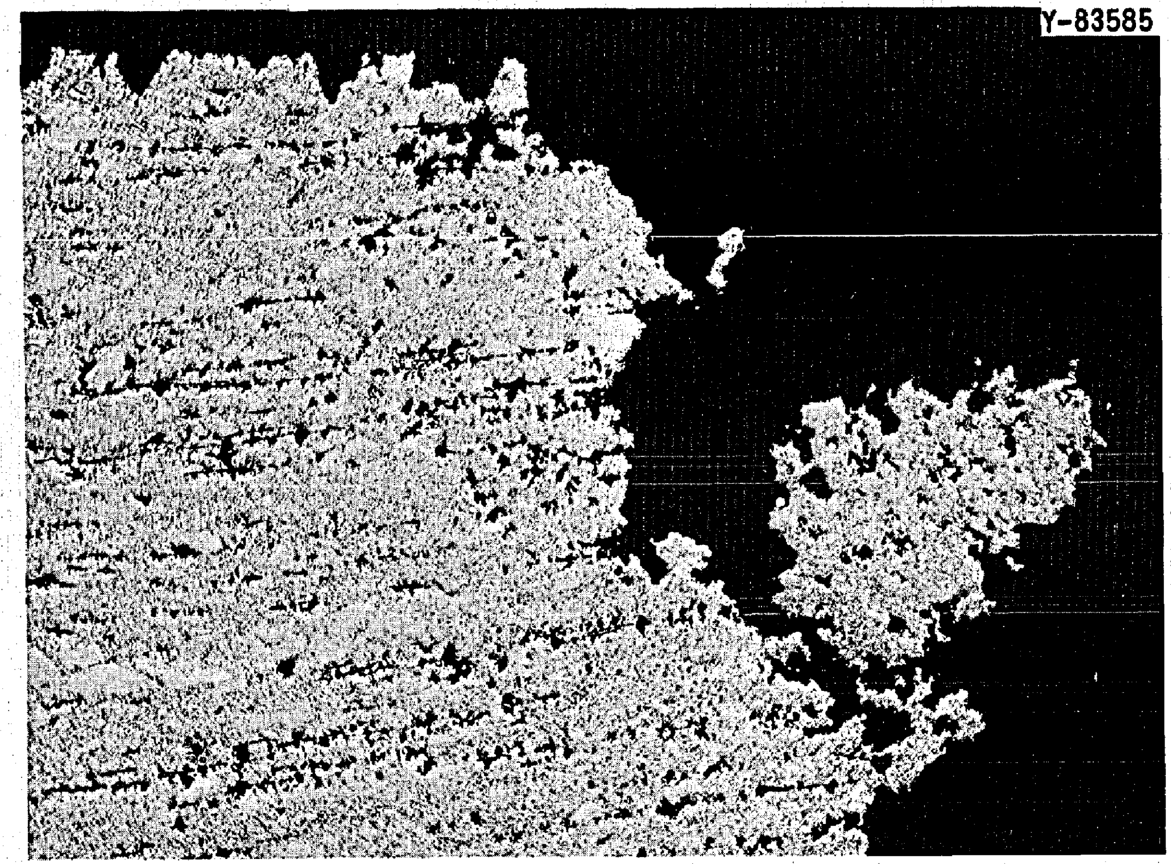

Fig. 39. Photomicrograph Showing the Fracture of a Zirconium-Modified Hastelloy N Sample (Heat 21554) Tested at 850°C at a Strain Rate of 0.002 $\min^{-1}$. Exposed to static fluoride salt for 5500 hr at 650°C before testing. Note the extensive grain boundary migration. 100×. Etchant: Glyceria regia.

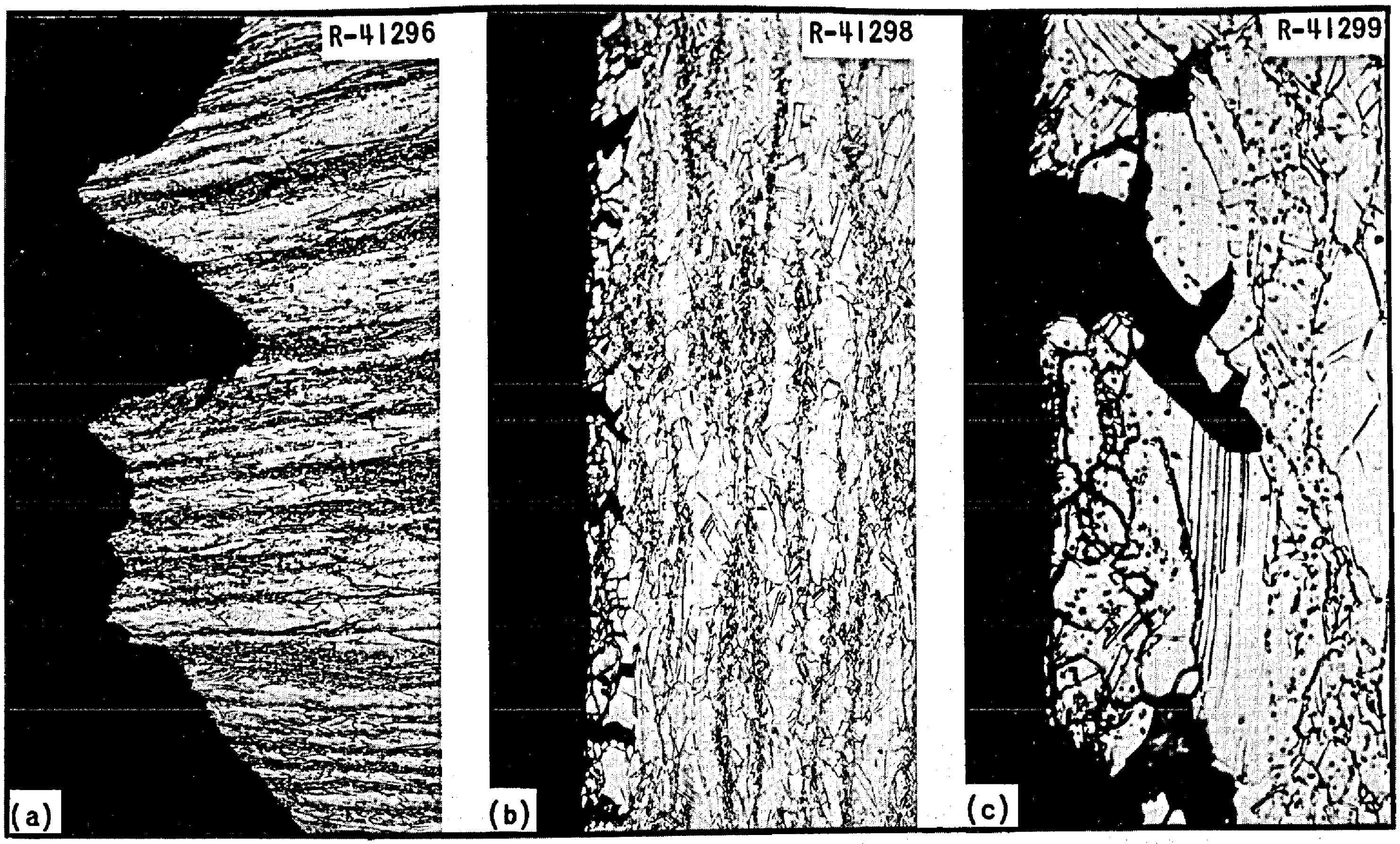

Fig. 40. Photomicrographs of a Titanium-Modified Hastelloy N Surveillance Sample (Heat 21545) Tested at 25°C at a Strain Rate of 0.05 min^{-1}. Exposed in the MSRE core for 5500 hr at 650°C to a thermal fluence of 4.1×10^{20} $neutrons/cm^2$. Etchant: Aqua regia. (a) Fracture. 100×. (b) Edge of sample about 1/2 in. from fracture. 100×. (c) Edge of sample showing edge cracking. 500×.

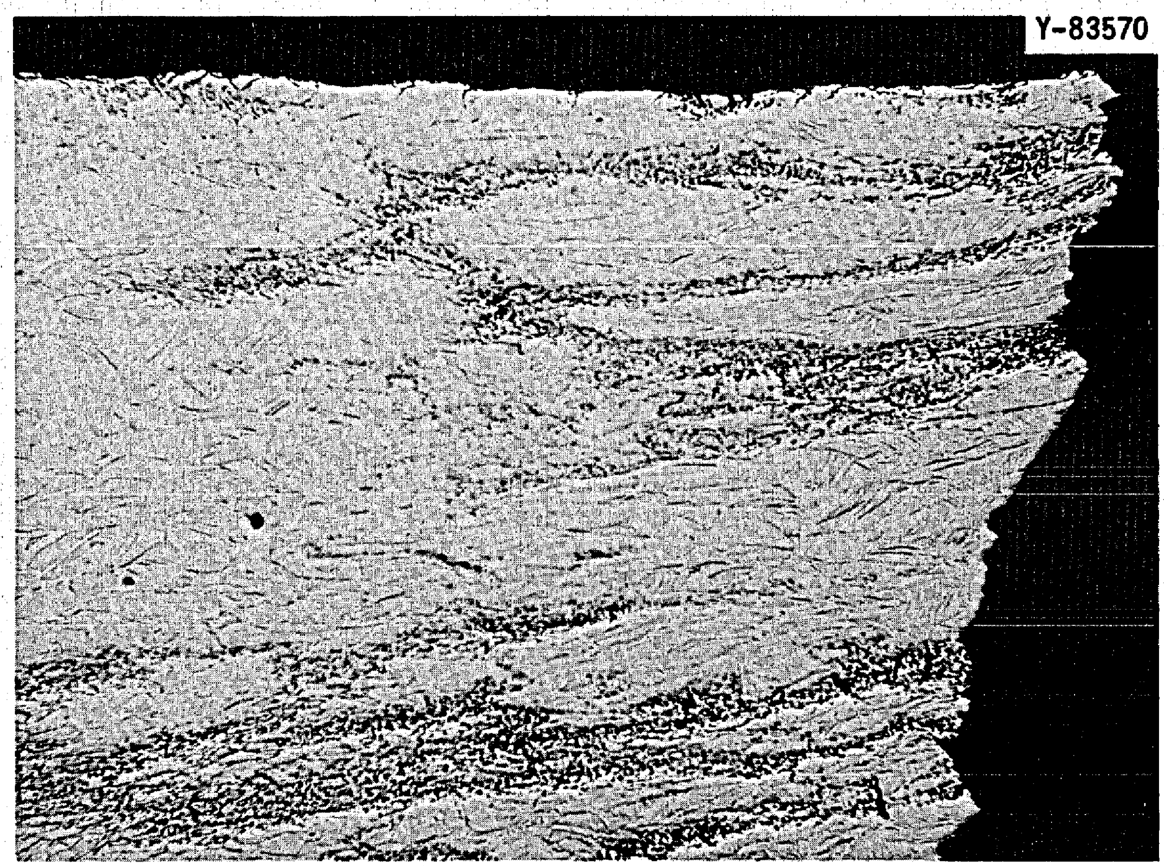

Fig. 41. Photomicrograph of the Fracture of a Titanium-Modified Hastelloy N Surveillance Sample (Heat 21545) Tested at 25°C at a Strain Rate of 0.05 min^{-1}. Exposed to a static fluoride salt for 5500 hr at 650°C before testing. Note the shear fracture and the absence of edge cracking. 100×. Etchant: Glyceria regia.

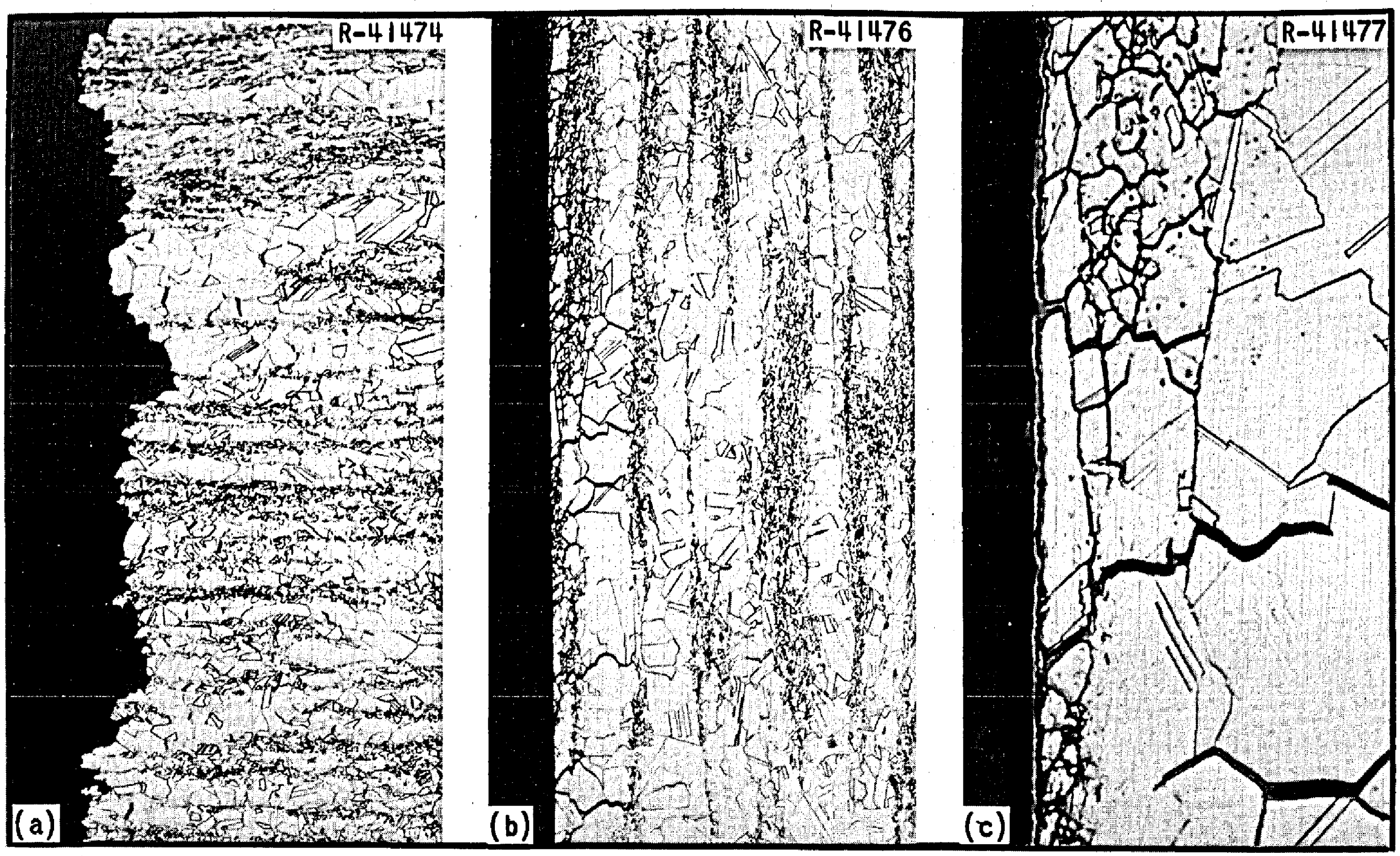

Fig. 42. Photomicrographs of a Titanium-Modified Hastelloy N Surveillance Sample (Heat 21545) Tested at 650°C at a Strain Rate of 0.002 min^{-1}. Exposed in the MSRE core for 5500 hr at 650°C to a thermal fluence of 4.1×10^{20} $neutrons/cm^2$. Etchant: Aqua regia. (a) Fracture. 100×. (b) Edge of sample about 1/2 in. from fracture. 100×. (c) Edge of sample showing edge cracking. Oxide formed during the tensile test. 500×.

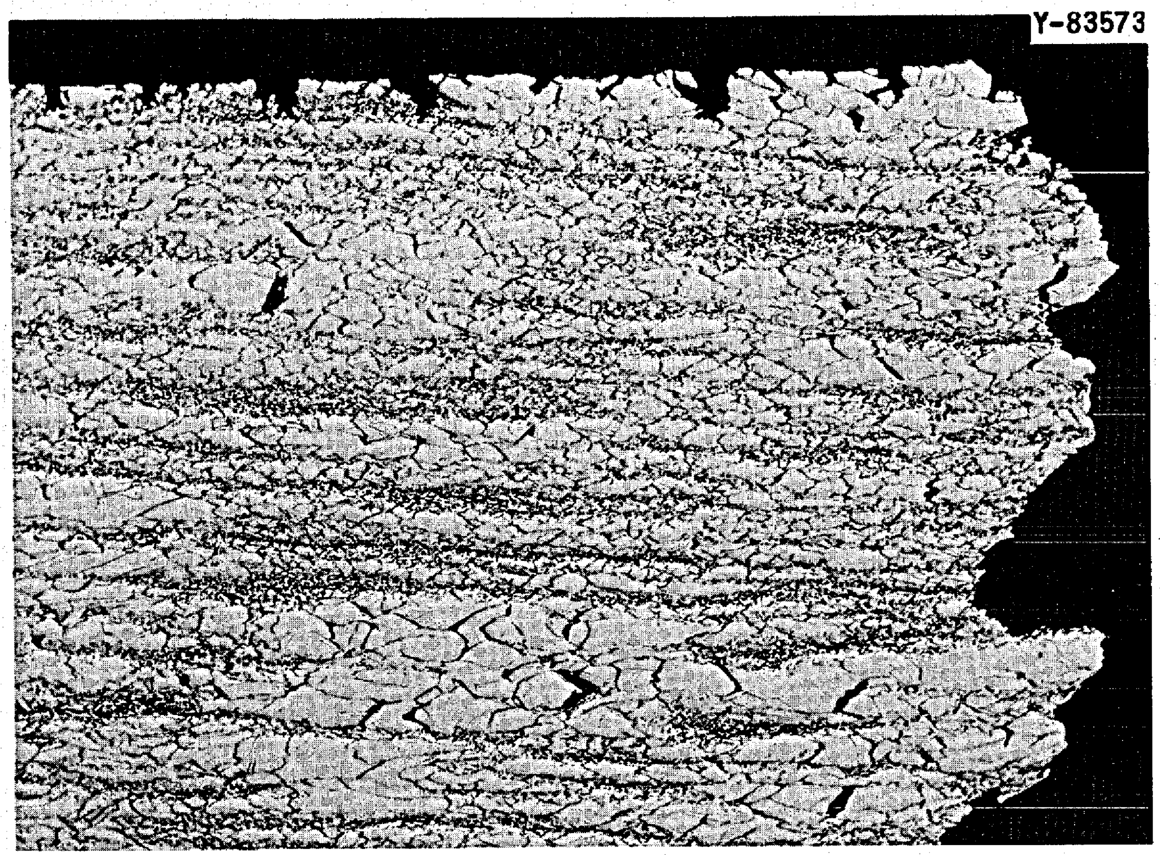

Fig. 43. Photomicrograph Showing a Portion of the Fracture of a Titanium-Modified Hastelloy N Surveillance Sample (Heat 21545) Tested at 650°C at a Strain Rate of 0.002 min^{-1}. Exposed to static fluoride salt for 5500 hr at 650°C before testing. 100×. Etchant: Glyceria regia.

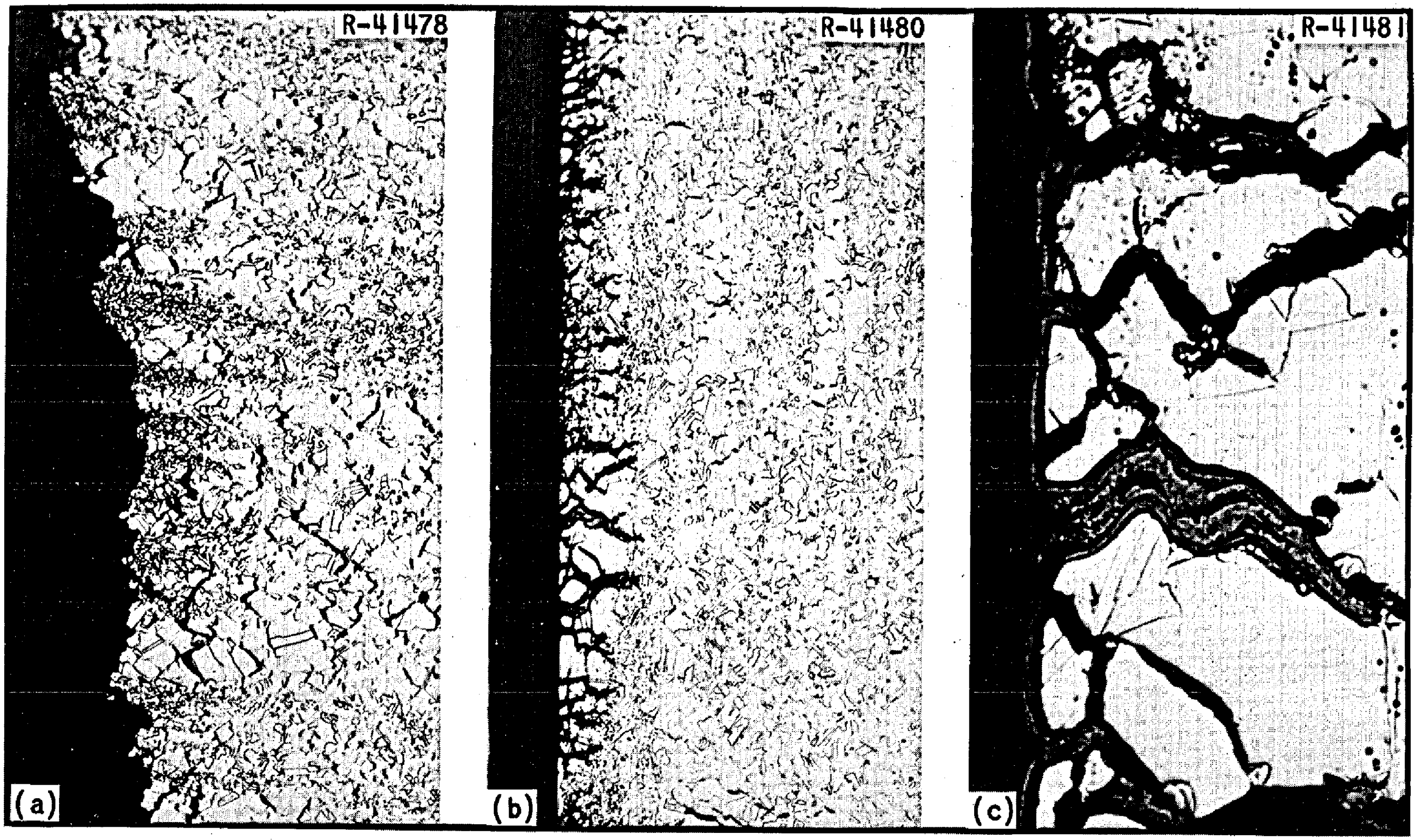

Fig. 44. Photomicrographs of a Titanium-Modified Hastelloy N Surveillance Sample (Heat 21545) Tested at 850°C at a Strain Rate of 0.002 min^{-1}. Exposed in the MSRE core for 5500 hr at 650°C to a thermal fluence of 4.1×10^{20} neutrons/cm^2. Etchant: Aqua regia. (a) Fracture. 100×. (b) Edge of sample about 1/2 in. from fracture. 100×. (c) Edge of sample showing edge cracking. Oxide formed during the tensile test. 500×.

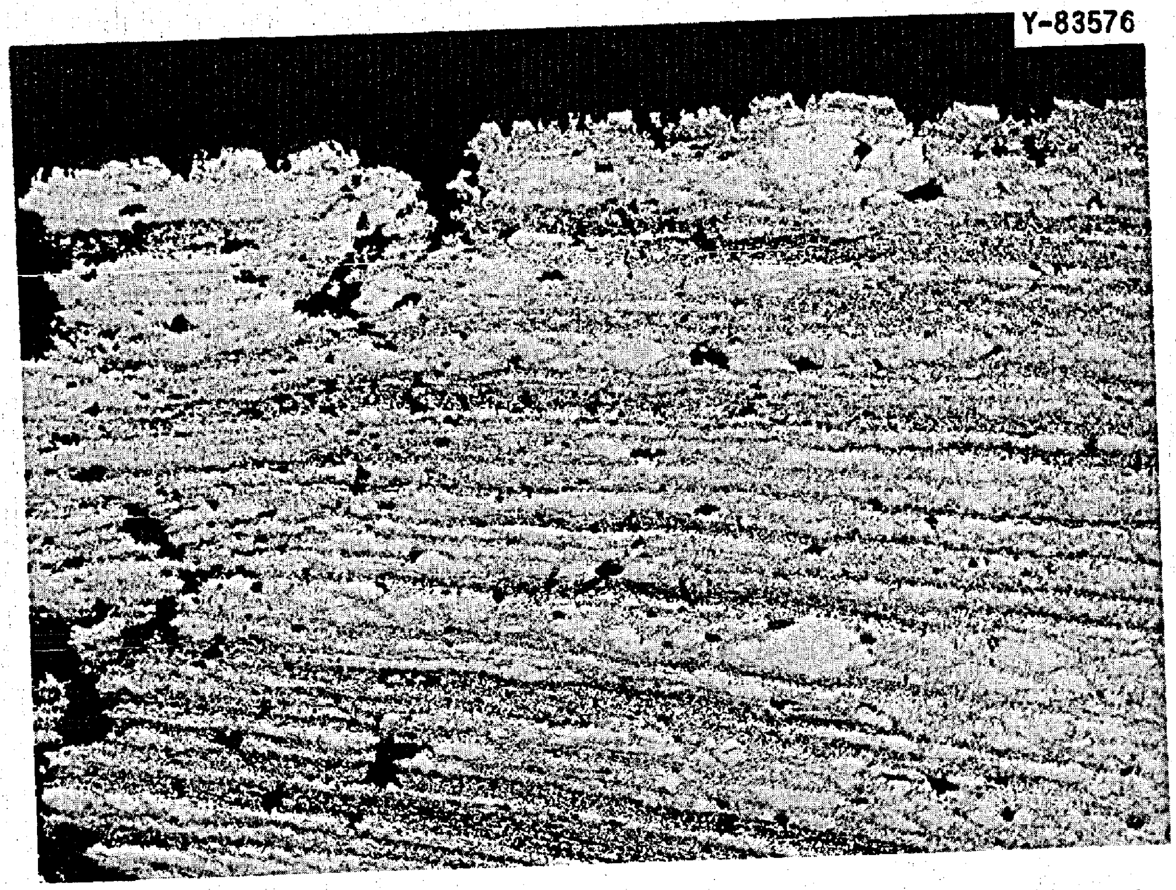

Fig. 45. Photomicrograph of the Fracture of a Titanium-Modified Hastelloy N Surveillance Sample (Heat 21545) Tested at 25°C at a Strain Rate of 0.05 min^{-1}. Exposed to a static fluoride salt for 5500 hr at 650°C before testing. Note the shear fracture and the absence of edge cracking. 100×. Etchant: Glyceria regia.

irradiated material, a completely intergranular fracture of the irradiated material at 650°C compared with a mixed transgranular and intergranular fracture in the unirradiated material, and grain boundary migration at a test temperature of 850°C.

DISCUSSION OF RESULTS

The standard Hastelloy N used in constructing the MSRE continues to show excellent compatibility with the fluoride salt environment and the cell environment consisting of N_2–2 to 5% O_2. There was no evidence of nitriding, and the depth of oxidation in 11,000 hr was only a few mils. We knew from previous studies that the mechanical properties of Hastelloy N would deteriorate due to irradiation damage.[12–17] Our examination of the first group of surveillance specimens[18] showed that the property changes were as-predicted, the only exception being a reduction in the ductility at 25°C. Extraction replicas showed that extensive carbide precipitation occurred along the grain boundaries during irradiation at 650°C, and this probably accounts for the reduction in ductility at 25°C.

Our primary purpose in this program is to continually assess the condition of the MSRE core vessel. The surveillance facility in the core

---

[12] H. E. McCoy, Jr., and J. R. Weir, Jr., Materials Development for Molten-Salt Breeder Reactors, ORNL-TM-1854 (June 1967).

[13] W. R. Martin and J. R. Weir, "Effect of Elevated Temperature Irradiation on the Strength and Ductility of the Nickel-Base Alloy, Hastelloy N," Nucl. Appl. 1(2), 160–167 (1965).

[14] W. R. Martin and J. R. Weir, "Postirradiation Creep and Stress-Rupture of Hastelloy N," Nucl. Appl. 3(3), 167 (1967).

[15] H. E. McCoy, Jr., and J. R. Weir, Jr., "Stress-Rupture Properties of Irradiated and Unirradiated Hastelloy N Tubes," Nucl. Appl. 4(2), 96 (1968).

[16] H. E. McCoy, Jr., Effects of Irradiation on the Mechanical Properties of Two Vacuum-Melted Heats of Hastelloy N, ORNL-TM-2043 (January 1968).

[17] H. E. McCoy, Jr., and J. R. Weir, Jr., In- and Ex-Reactor Stress-Rupture Properties of Hastelloy N Tubing, ORNL-TM-1906 (September 1967).

[18] H. E. McCoy, Jr., An Evaluation of the Molten-Salt Reactor Experiment Hastelloy N Surveillance Specimen — First Group, ORNL-TM-1997 (November 1967).

receives a thermal flux about a factor of 40 higher than that received by the vessel. The first surveillance specimens removed from the core received a thermal fluence of 1.3×10^{20} neutrons/cm^2 while being heated for 4800 hr. The surveillance specimens of standard Hastelloy N removed with the second group were located outside the core and received a thermal fluence of 1.3×10^{19} neutrons/cm^2 while being heated for 11,000 hr. The latter group should indicate more closely the properties of the vessel, but a comparison of the properties of both groups is important in trying to estimate the future properties. The fracture strain in tensile tests (Fig. 14, p. 25) is reduced even more by the higher fluence. In creep-rupture tests at 650°C (Fig. 15, p. 27), the rupture life is also slightly shorter and the strain at fracture (Fig. 17, p. 29) slightly less for the specimen irradiated to the higher fluence. In the unirradiated condition, heat 5085 exhibited fracture strains of 20 to 40% in creep-rupture tests compared with fracture strains of about 2.2 and 1.5% after irradiation to thermal fluences of 1.3×10^{19} neutrons/cm^2 and 1.3×10^{20} neutrons/cm^2, respectively. Thus, even though the properties continue to change slightly with increasing fluence, the rate of change has decreased markedly.

Another encouraging observation is that the MSRE materials do not seem to have as low minimum fracture strains after irradiation as we have noted for the same materials after irradiation to the same fluences in the ORR (Fig. 17, p. 29). This may be due to the more extensive carbide precipitation in the materials irradiated in the MSRE for long periods of time.

The modified alloys, heats 21554 (zirconium modified) and 21545 (titanium modified), were annealed to produce a small grain size. Since these samples were placed in the MSRE, we have found that material annealed to produce a coarser grain size has better properties after irradiation.[19] Thus, we were not surprised that the postirradiation

---

[19]H. E. McCoy and J. R. Weir, "Development of a Titanium-Modified Hastelloy with Improved Resistance to Radiation Damage," paper presented at the Symposium on Effects of Radiation on Structural Metals, American Society for Testing and Materials, San Francisco, California, June 23–28, 1968. To be published in the proceedings.

properties of the modified alloys were not much better than those observed for the standard Hastelloy N. However, two encouraging observations were made that demonstrate the absence of embrittling aging reactions: (1) the mechanical properties of the control specimens exposed to salt for 5500 hr were only slightly different from those of the as-annealed material (Figs. 24 and 25, pp. 38 and 41) and (2) the strain at fracture in tensile tests at 25°C was not reduced by irradiation. The most disturbing observation is the intergranular cracking near the surface of specimens that were removed from the reactor. Our measurements[20] of the lattice diffusion of titanium in the modified alloy indicate that the gradients in these samples should extend to a depth of only about 0.15 mil (based on a lattice diffusion coefficient of 1×10^{-15} cm^2/sec and 5500 hr exposure at 650°C). However, titanium can diffuse more rapidly along the grain boundaries and we can approximate this depth of removal by the Fisher model.[21] Assuming that the grain boundary diffusion rate is 10^6 times that for the lattice,[22] significant depletion of the titanium should occur along the grain boundaries to depths of about 4 mils. This is in reasonable agreement with the depth of the surface cracks observed in the surveillance specimens (Figs. 34 and 40, pp. 50 and 56). However, the control specimens (Figs. 35 and 41, pp. 51 and 57) were exposed to static salt but did exhibit edge cracking when tested. It is possible that corrosion in the static vessel proceeds more slowly than in the flowing reactor circuit or that the grain boundary cracking may be a result of the loss or ingress of some element besides titanium.

SUMMARY AND CONCLUSIONS

We have examined the second group of surveillance samples removed from the MSRE. Two rods of standard Hastelloy N were removed from the

---

[20]C. E. Sessions and T. S. Lundy, "Diffusion of Titanium in Modified Hastelloy N," Molten-Salt Reactor Program Semiann. Progr. Rept. Feb. 29, 1968, ORNL-4254, pp. 213–215.

[21]J. C. Fisher, "Calculation of Diffusion Penetration Curves for Surface and Grain Boundary Diffusion," J. Appl. Phys. 22, 74 (1951).

[22]W. R. Upthegrove and M. J. Sinnott, "Grain Boundary Self-Diffusion of Nickel," Trans. Am. Soc. Metals 50, 1031 (1958).

surveillance position outside the core after 11,000 hr at temperature with a thermal fluence of 1.3×10^{19} neutrons/cm^2. The compatibility of the material with the cell environment of nitrogen plus 2 to 5% O_2 seems excellent with no evidence of nitriding and only superficial oxidation. Mechanical property tests show that the fracture strain at 25°C and above 500°C was reduced markedly by irradiation. Creep-rupture tests at 650°C show a reduction in rupture life and ductility. A comparison with results from the first group of surveillance specimens exposed to the core environment to a fluence of 1.3×10^{20} neutrons/cm^2 indicated that the mechanical properties deteriorated only slightly with increasing fluence.

Two heats of modified Hastelloy N containing 0.5% Ti and 0.5% Zr were removed from the core with a thermal fluence of 4.1×10^{20} neutrons/cm^2. They had not been annealed to obtain the optimum properties and their postirradiation mechanical properties were only slightly better than those observed for the standard alloy. However, these alloys did not seem to age and their corrosion resistance seems acceptable.

ACKNOWLEDGMENTS

The author is indebted to numerous persons for assistance in this study.

W. H. Cook and A. Taboada — Design of surveillance assembly and insertion of specimens.

W. H. Cook and R. C. Steffy — Flux measurements.

J. R. Weir, Jr., and W. H. Cook — Review of the manuscript.

E. J. Lawrence and J. L. Griffith — Assembled surveillance and control specimens in fixture.

P. Haubenreich and MSRE Operation Staff — Exercised extreme care in inserting and removing the surveillance specimens.

E. M. King and Hot Cell Operation Staff — Developed techniques for cutting long rods into individual specimens, determined specimen straightness, and offered assistance in running creep and tensile tests.

B. C. Williams, B. McNabb, N. O. Pleasant — Ran tensile and creep tests on surveillance and control specimens.

E. M. Thomas and J. Feltner — Processed test data.

J. A. Snyder and R. H. Jones — Developed technique for making Hastelloy N surveillance rods.

H. R. Tinch and E. Lee — Metallography on control and surveillance specimens.

W. C. Colwell, Jr., and Graphite Arts — Preparation of drawings.

Thelma Reedy and Meredith Hill, Metals and Ceramics Division Reports Office — Preparation of report.

INTERNAL DISTRIBUTION

1–3. Central Research Library
4–5. ORNL Y-12 Technical Library
Document Reference Section
6–25. Laboratory Records
26. Laboratory Records, ORNL-RC
27. ORNL Patent Office
28. R. K. Adams
29. G. M. Adamson
30. R. G. Affel
31. J. L. Anderson
32. R. F. Apple
33. C. F. Baes
34. J. M. Baker
35. S. J. Ball
36. C. E. Bamberger
37. C. J. Barton
38. H. F. Bauman
39. S. E. Beall
40. R. L. Beatty
41. M. J. Bell
42. M. Bender
43. C. E. Bettis
44. E. S. Bettis
45. D. S. Billington
46. R. E. Blanco
47. F. F. Blankenship
48. J. O. Blomeke
49. R. Blumberg
50. E. G. Bohlmann
51. C. J. Borkowski
52. G. E. Boyd
53. J. Braunstein
54. M. A. Bredig
55. R. B. Briggs
56. H. R. Bronstein
57. G. D. Brunton
58. D. A. Canonico
59. S. Cantor
60. W. L. Carter
61. G. I. Cathers
62. O. B. Cavin
63. A. Cepolina
64. J. M. Chandler
65. F. H. Clark
66. W. R. Cobb
67. H. D. Cochran
68. C. W. Collins
69. E. L. Compere
70. K. V. Cook
71. W. H. Cook
72. L. T. Corbin
73. B. Cox
74. J. L. Crowley
75. F. L. Culler
76. D. R. Cuneo
77. J. E. Cunningham
78. J. M. Dale
79. D. G. Davis
80. R. J. DeBakker
81. J. H. DeVan
82. S. J. Ditto
83. A. S. Dworkin
84. I. T. Dudley
85. D. A. Dyslin
86. W. P. Eatherly
87. J. R. Engel
88. E. P. Epler
89. D. E. Ferguson
90. L. M. Ferris
91. A. P. Fraas
92. H. A. Friedman
93. J. H Frye, Jr.
94. W. K. Furlong
95. C. H. Gabbard
96. R. B. Gallaher
97. R. E. Gehlbach
98. J. H. Gibbons
99. L. O. Gilpatrick
100. W. R. Grimes
101. A. G. Grindell
102. R. W. Gunkel
103. R. H. Guymon
104. J. P. Hammond
105. B. A. Hannaford
106. P. H. Harley
107. D. G. Harman
108. W. O. Harms
109. C. S. Harrill
110. P. N. Haubenreich
111. R. E. Helms
112. P. G. Herndon
113. D. N. Hess

114. J. R. Hightower
115–117. M. R. Hill
118. H. W. Hoffman
119. D. K. Holmes
120. P. P. Holz
121. R. W. Horton
122. A. Houtzeel
123. T. L. Hudson
124. W. R. Huntley
125. H. Inouye
126. W. H. Jordan
127. P. R. Kasten
128. R. J. Kedl
129. M. T. Kelley
130. M. J. Kelly
131. C. R. Kennedy
132. T. W. Kerlin
133. H. T. Kerr
134. J. J. Keyes
135. D. V. Kiplinger
136. S. S. Kirslis
137. J. W. Koger
138. R. B. Korsmeyer
139. A. I. Krakoviak
140. T. S. Kress
141. J. W. Krewson
142. C. E. Lamb
143. J. A. Lane
144. C. E. Larson
145. J. J. Lawrence
146. M. S. Lin
147. R. B. Lindauer
148. A. P. Litman
149. G. H. Llewellyn
150. E. L. Long, Jr.
151. A. L. Lotts
152. M. I. Lundin
153. R. N. Lyon
154. R. L. Macklin
155. H. G. MacPherson
156. R. E. MacPherson
157. J. C. Mailen
158. D. L. Manning
159. C. D. Martin
160. W. R. Martin
161. H. V. Mateer
162. T. H. Mauney
163. H. McClain
164. R. W. McClung
165. H. E. McCoy
166. D. L. McElroy
167. C. K. McGlothlan
168. C. J. McHargue
169. L. E. McNeese
170. J. R. McWherter
171. H. J. Metz
172. A. S. Meyer
173. R. L. Moore
174. D. M. Moulton
175. T. W. Mueller
176. H. A. Nelms
177. H. H. Nichol
178. J. P. Nichols
179. E. L. Nicholson
180. E. D. Nogueira
181. L. C. Oakes
182. P. Patriarca
183. A. M. Perry
184. T. W. Pickel
185. H. B. Piper
186. B. E. Prince
187. G. L. Ragan
188. J. L. Redford
189. M. Richardson
190. G. D. Robbins
191. R. C. Robertson
192. W. C. Robinson
193. K. A. Romberger
194. R. G. Ross
195. H. C. Savage
196. W. F. Schaffer
197. C. E. Schilling
198. Dunlap Scott
199. J. L. Scott
200. H. E. Seagren
201. C. E. Sessions
202. J. H. Shaffer
203. W. H. Sides
204. G. M. Slaughter
205. A. N. Smith
206. F. J. Smith
207. G. P. Smith
208. O. L. Smith
209. P. G. Smith
210. I. Spiewak
211. R. C. Steffy
212. W. C. Stoddart
213. H. H. Stone
214. R. A. Strehlow
215. D. A. Sundberg
216. J. R. Tallackson
217. E. H. Taylor
218. W. Terry
219. R. E. Thoma

220. P. F. Thomason
221. L. M. Toth
222. D. B. Trauger
223. W. E. Unger
224. G. M. Watson
225. J. S. Watson
226. H. L. Watts
227. C. F. Weaver
228. B. H. Webster
229. A. M. Weinberg
230. J. R. Weir
231. W. J. Werner
232. K. W. West
233. M. E. Whatley
234. J. C. White
235. R. P. Wichner
236. L. V. Wilson
237. Gale Young
238. H. C. Young
239. J. P. Young
240. E. L. Youngblood
241. F. C. Zapp

EXTERNAL DISTRIBUTION

242. G. G. Allaria, Atomics International
243. J. G. Asquith, Atomics International
244. D. F. Cope, RDT, SSR, AEC, Oak Ridge National Laboratory
245. C. B. Deering, AEC, OSR, Oak Ridge National Laboratory
246. H. M. Dieckamp, Atomics International
247. A. Giambusso, AEC, Washington
248. F. D. Haines, AEC, Washington
249. C. E. Johnson, AEC, Washington
250. W. L. Kitterman, AEC, Washington
251. W. J. Larkin, AEC, Oak Ridge Operations
252–253. T. W. McIntosh, AEC, Washington
254. A. B. Martin, Atomics International
255. D. G. Mason, Atomics International
256. G. W. Meyers, Atomics International
257. D. E. Reardon, AEC, Canoga Park Area Office
258. H. M. Roth, AEC, Oak Ridge Operations
259. M. Shaw, AEC, Washington
260. J. M. Simmons, AEC, Washington
261. W. L. Smalley, AEC, Washington
262. S. R. Stamp, AEC, Canoga Park Area Office
263. E. E. Stansbury, the University of Tennessee
264. D. K. Stevens, AEC, Washington
265. R. F. Sweek, AEC, Washington
266. A. Taboada, AEC, Washington
267. R. F. Wilson, Atomics International
268. Laboratory and University Division, AEC, Oak Ridge Operations
269–283. Division of Technical Information Extension